

## *L*-shell Coulomb ionization by heavy charged particles

Werner Brandt and Grzegorz Lapicki

*Department of Physics, New York University, New York, New York 10003*

(Received 16 January 1979)

The theory of Coulomb ionization of *L* shells by low-velocity heavy charged particles whose atomic number is small compared to the atomic number of the target atom is extended to projectiles with velocities comparable to or larger than the *L*-shell orbital velocities. At large impact parameters projectiles polarize the shell, and at small impact parameters they increase the binding energies of the electrons to be excited. The polarization effect is incorporated in accordance with the perturbed stationary-state (PSS) approximation. The effect of the repulsion between the projectile and the target nucleus is accounted for by a Coulomb-deflection factor (C). This CPSS theory is developed further to include relativistic effects (R) of the target wave function through a procedure that reproduces the results of numerical calculations for heavy target atoms. With electron capture by the projectiles as an additional channel of ionization, the CPSSR theory is compared with experiment.

### I. INTRODUCTION

Inelastic collisions of charged projectiles with atoms create inner-shell vacancies. If the projectiles are charged elementary particles which are heavier than the electron, or if they are ions whose atomic number  $Z_1$  is small compared to the target atomic number  $Z_2$ , then Coulomb excitation dominates the inner-shell vacancy production through (direct) ionization to the continuum of the target atom, or by electron capture into an unoccupied state of the projectile. Our approach casts the theory of inner-shell ionization into a comprehensive form which allows for the mutual perturbation of the projectile and target states during the collision.<sup>1</sup>

In previous papers we developed the theory for the direct Coulomb ionization of *K* shells<sup>2,3</sup> and of *L* subshells<sup>4</sup> by heavy charged particles of low velocities in comparison to the orbital velocities. We resolved order-of-magnitude discrepancies between the predictions of the plane-wave Born approximation<sup>5,6</sup> (PWBA) or the equivalent semiclassical approximation<sup>7</sup> (SCA) with straight trajectories, and experimental ionization cross sections. This was accomplished by incorporating into the theory two effects not included in the PWBA. They are<sup>1-4</sup> (i) the Coulomb repulsion (C) of the projectile by the target nucleus that leads to its retardation and deflection from a straightline trajectory during the collision, and (ii) the increase in the binding energy of the inner-shell electron to be ionized due to the proximity of the ionizing particle. A multiplicative Coulomb-deflection factor for the cross section was extracted<sup>2</sup> from the semiclassical calculations of Bang and Hansteen.<sup>7</sup> Increased binding was incorporated<sup>2</sup> in a manner equivalent to an *ab initio* calculation in the framework of the perturbed

stationary-state (PSS) theory.<sup>8</sup> This approach including Coulomb repulsion and perturbed stationary states (CPSS) was cast in terms of the PWBA cross sections that were derived with nonrelativistic target wave functions for the description of inner-shell electrons.<sup>1-4</sup>

We now extend this work to *L*-shell ionizations at intermediate projectile velocities. Furthermore, we incorporate the relativistic effect in the description of the target states and assess the status of the Coulomb-deflection effect. The projectiles are taken to move nonrelativistically, i.e., to be of kinetic energy per mass less than 50 MeV/amu.<sup>9</sup> Atomic units are used hereafter, except in the figures and Appendix B. Section II reviews the PWBA based on nonrelativistic wave functions and introduces a procedure which duplicates the plane-wave Born approximation (PWBA) inner-shell results based on relativistic (R) wave functions.<sup>10-12</sup> Section III derives the polarization effect for a harmonic oscillator model of atomic states and combines it with the binding effect to yield the PSS result. The Coulomb-deflection effect is reconsidered in Sec. IV. With the addition of electron-capture contributions,<sup>13</sup> the CPSSR cross sections as derived here are compared, in Sec. V, with experiment. Appendix A treats the Coulomb-deflection factor in the monopole approximation to the perturbing potential. Appendix B delineates an illustrative sample calculation of x-ray-production cross sections for *L* shells.

### II. RELATIVISTIC EFFECT IN THE PLANE-WAVE BORN APPROXIMATION (PWBA)

Consider the ionization of an inner shell *S* of a target atom bombarded by a heavy projectile of mass  $M_1 \gg 1$ . For the target (subscript 2), the *K* and *L* states are characterized by the quantum

numbers  $S \equiv (n_2, l_2, j_2)$  as  $K \equiv (1, 0, \frac{1}{2})$ ,  $L_1 \equiv (2, 0, \frac{1}{2})$ ,  $L_2 \equiv (2, 1, \frac{1}{2})$ , and  $L_3 \equiv (2, 1, \frac{3}{2})$ . The  $K$ -shell ionization theory and its nonrelativistic predictions have been discussed elsewhere.<sup>1-3, 14</sup> We approach  $K$ - and  $L$ -shell ionization in a unified manner, but compare its results mainly with  $L$ -shell data.

In the PWBA the projectile is described by a plane wave, and we represent the target atom by a product of screened-hydrogenic (SH) wave functions. There is ample evidence that products of single-electron wave functions,<sup>15</sup> and, specifically, of SH wave functions,<sup>5</sup> give  $K$ -shell ionization cross sections that agree within a few percent with those calculated based on Hartree-Slater (HS) wave functions.<sup>3, 16</sup> Products of single-electron wave functions also appear to suffice for the calculation of  $L$ -shell cross sections, although differential cross sections based on SH wave functions were found to be larger by a factor of 2-5 than those calculated with HS wave functions at small energy transfer,<sup>17-19</sup> corresponding to high projectile velocities or large impact parameters where deviations from a hydrogenic picture can be expected. Still, we find that the integrated cross sections differ by no more than  $\sim 35\%$  in  $^{13}\text{Al}(L)$ , and that the variation with the choice of wave function diminishes rapidly with increasing  $Z_2$ . For  $^{18}\text{Ar}(L)$  it amounts to only a few percent except at the highest velocity studied where it is about 10%.<sup>20</sup> Moreover, electron correlations, which are inherently not included in the Hartree-Slater approach, tend to close the gap between calculations with HS and SH wave functions.<sup>21</sup>

In terms of the screened nuclear charges,  $Z_{2K} = Z_2 - 0.3$  and  $Z_{2Li} = Z_{2L} = Z_2 - 4.15$ , the  $S$ -shell radius, orbital velocity, and binding energy are  $a_{2S} = n_2^2 / Z_{2S}$ ,  $v_{2S} = Z_{2S} / n_2$ , and  $\omega_{2S} = \frac{1}{2} \theta_S v_{2S}^2$ , respectively. If  $\omega_{2S}$  is equated to the observed binding energy,<sup>22</sup> the reduced binding energy  $\theta_S$  ranges from 0.6 to 1.0 for the  $K$  shells and from 0.4 to 0.8 for the  $L$  shells. As long as the projectile energy loss  $\sim \omega_{2S}$  in the ionization process is small compared to its kinetic energy  $E_1$ , one may write the nonrelativistic PWBA cross section for direct ionization of an  $S$  shell as<sup>4</sup>

$$\sigma_S^{\text{PWBA}}(\xi_S, \theta_S) = \frac{(2j_2 + 1)4\pi a_{2S}^2 (Z_1/Z_{2S})^2 F_S(\xi_S, \theta_S)}{\theta_S}, \quad (1)$$

where  $F_S(\xi_S, \theta_S)$  are tabulated functions<sup>3, 4, 14, 21</sup> based on the tables of Ref. 6. The minimum momentum transfer to an  $S$ -shell electron from a particle of velocity  $v_1$ ,  $q_{0S} \approx \frac{1}{2} \theta_S v_{2S}^2 / v_1$ , determines the variable

$$\xi_S \equiv n_2 / q_{0S} a_{2S} = v_1 / \frac{1}{2} \theta_S v_{2S}, \quad (2)$$

which distinguishes slow collisions, when  $\xi_S < 1$ , from those that occur in times comparable or shorter than the characteristic  $S$ -shell orbital time  $\sim a_{2S} / v_{2S}$ . Analytical forms for  $F_S$  at low velocities are given by Eqs. (7)-(9) of Ref. 4. They apply for  $\xi_S \ll 1$ , but with a lower bound  $\sim 0.15 / (M_1 \theta_S)^{1/2}$  if one posits  $\omega_{2S} / E_1 \lesssim 0.1$  as a limit of small energy loss.

As was noted already a quarter century ago,<sup>23</sup> a relativistic description of inner shells should increase the ionization cross sections in slow collisions. The relativistic effect has, in the meantime, been investigated for  $K$ -shell ionization,<sup>24</sup> but only a few complete calculations with relativistic wave functions were performed in the PWBA<sup>10, 11</sup> and in the SCA for straight-line<sup>12</sup> and hyperbolic<sup>25</sup> trajectories. Various schemes were proposed to reproduce this effect without involved numerical calculations.<sup>21, 26-30</sup> Following Hönl,<sup>31</sup> Merzbacher and Lewis<sup>26</sup> suggested that one should continue to employ the cross sections based on nonrelativistic screened hydrogenic wave functions but with  $\theta_S$  reduced to  $\theta_S^R = \theta_S - (v_{2S}/c)^2 [n_2 / (j_2 + \frac{1}{2}) - \frac{3}{4}]$ ,  $c \approx 137$  being the velocity of light. It has been argued<sup>21, 30</sup> that a change of  $\theta_S$  to  $\theta_S^R = \theta_S / \{1 + (v_{2S}/c)^2 [n_2 / (j_2 + \frac{1}{2}) - \frac{3}{4}]\}$  would be more appropriate, although such a prescription gives only slightly lower values of  $\theta_S^R$ . Hardt and Watson<sup>27</sup> proposed instead to decrease the orbital velocity  $v_{2S}$  in accord with the relativistic expression for the mean kinetic energy in the virial theorem. Recently, Berinde *et al.*<sup>32</sup> incorporated the relativistic effect for  $K$ -shell ionization by replacing  $a_{2K}$  with  $a_{2K}(1 - v_{2K}^2/c^2)^{1/2}$  in  $\xi_S$ , Eq. (2).

Such approximate methods are inadequate since they mimic the relativistic effect by a change of the average quantities that characterize inner shells; such approaches can reproduce numerical calculations with relativistic wave functions only when  $v_1 \approx v_{2S}$  and the important impact parameters in the collision are comparable to  $a_{2S}$ . When ionization takes place deep inside the inner shell, the relativistic effect can become significant even for  $L$  shells of light atoms. A relativistic change in the binding energy, the mean velocity, or the radius of the electron orbit grossly underestimates this effect. Hansen<sup>28</sup> approximates the relativistic electron-momentum distribution for use in the binary encounter approximation (BEA). It is, however, not possible to apply this procedure straightforwardly in the PWBA. Hansen's corrections, presented as a table of  $(\sigma_K^R / \sigma_K)^{\text{BEA}}$  for different projectile velocities and target atoms, still underestimate the relativistic effect in the slow collision regime when compared with  $(\sigma_K^R / \sigma_K)^{\text{PWBA}}$ , where  $\sigma_K^R$  is computed with relativistic wave functions.

Recently, Amundsen *et al.*<sup>12,29</sup> and Anholt<sup>33</sup> extracted various analytical factors for *K*-shell ionization from an SCA approximation with relativistic wave functions. Their use appears to be restricted to low projectile velocities.

In what follows, we develop a relativistic correction to  $\sigma_S^{\text{PWBA}}$  in a manner analogous to the way in which we account for the binding effect.<sup>1-4</sup> In the low-velocity limit,<sup>34</sup>  $\xi_S \ll 1$ , the ionization cross section is proportional to the fourth power of

$$T_{\text{max}} = 2mv_1^2 = m\theta_S \omega_{2S} \xi_S^2, \quad (3)$$

the maximum energy transferred from the projectile to an electron of mass  $m$ . Instead of setting  $m=1$ , however, we calculate  $T_{\text{max}}$  by introducing a "local" relativistic electron mass through the virial theorem<sup>35</sup> for a relativistic electron in a central potential. In a potential of the form  $Z_{2S}/r$  at the distance  $r$  from the target nucleus, this mass  $m^R(r)$  is

$$m^R(r) = [1 + (Z_{2S}/2rc^2)^2]^{1/2} + Z_{2S}/2rc^2. \quad (4)$$

We choose for  $1/r$  in this equation a mean value  $\langle 1/R(t) \rangle \equiv (\alpha p)^{-1}$  of the inverse of the projectile

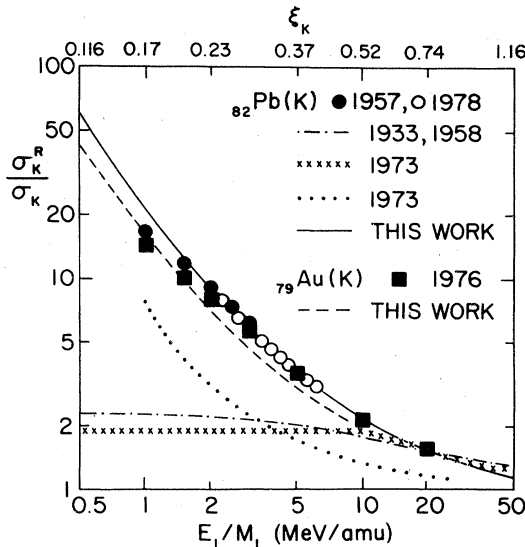


FIG. 1. Ratios of theoretical cross sections in PWBA calculated with relativistic and nonrelativistic *K*-shell wave functions of lead and gold. The solid symbols show the results of Ref. 10 (● 1957) and Ref. 12 (■ 1976). The open circles are results from Ref. 25 based on a semiclassical approach with hyperbolic trajectories (○ 1978). Curves represent ratios based on schemes which account for the relativistic effect in various approximate ways, viz., according to Refs. 26 and 31 (—·— 1958, 1933), Ref. 27 (xxxxx 1973), and Ref. 28 (····· 1973). Our results, calculated according to Eq. (7), are given by the curve — for  $_{82}\text{Pb}$  and the curve — — — for  $_{79}\text{Au}$ .

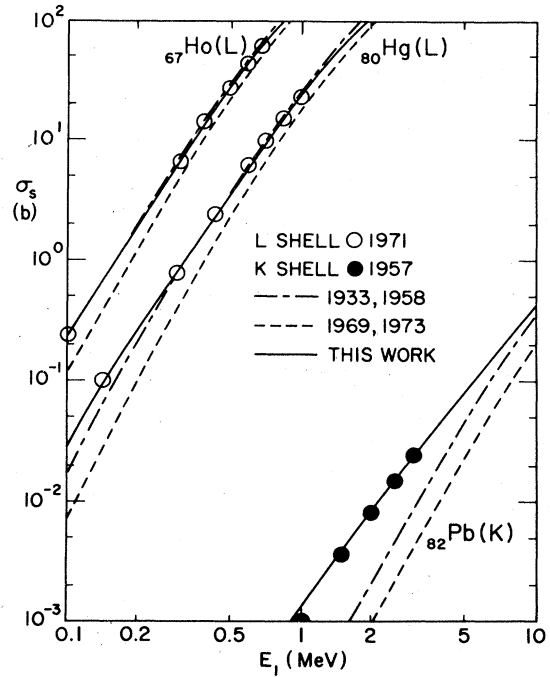


FIG. 2. Calculated *K*-shell and *L*-shell ionization cross sections in the PWBA with relativistic wave functions [Ref. 10 for  $_{82}\text{Pb}$  (*K*) (● 1957) and Ref. 11 for  $_{67}\text{Ho}$  (*L*) and  $_{80}\text{Hg}$  (*L*) (○ 1971)] and with nonrelativistic wave functions (Ref. 6 — — — 1969, 1973). The results of Hönl's procedure (Refs. 26 and 31 — · — 1958, 1933) and of our calculations based on Eq. (7) (—) are shown for comparison.

distance to the target nucleus,  $R(t) \equiv (p^2 + v_1^2 t^2)^{1/2}$ , where  $p$  is the impact parameter,

$$\begin{aligned} \frac{1}{\alpha p} &= \left\langle \frac{1}{R(t)} \right\rangle = \frac{1}{\alpha p} \int_0^{\alpha p} \frac{d(v, t)}{(p^2 + v_1^2 t^2)^{1/2}} \\ &= \frac{1}{\alpha p} \operatorname{arcsinh} \alpha, \end{aligned}$$

which determines the constant  $\alpha = \sinh 1 = 1.1752$ . On averaging Eq. (4) over all impact parameters with the weight functions  $W_S$  defined in Ref. 4,

$$m_S^R(\xi_S) = \int_0^\infty m^R(\alpha p) W_S(p q_{0S}) p q_{0S} d(p q_{0S}), \quad (5)$$

one obtains<sup>36</sup>

$$m_S^R(\xi_S) \simeq (1 + \beta y_S^2)^{1/2} + y_S, \quad (6)$$

where

$$y_{K, L_1} \equiv \frac{0.40(Z_{2S}/c)^2}{n_2 \xi_{K, L_1}}, \quad y_{L_2, L_3} \equiv \frac{0.15(Z_{2L}/c)^2}{\xi_{L_2, L_3}},$$

and  $\beta$  is a slowly varying parameter. Equation (6) with  $\beta = 1.1$  agrees with the numerical integration

of Eq. (5) to within 3% over the relevant  $\xi_s$  range. Equation (3) implies a transformation from  $\xi_s$ , Eq. (2), to  $[m_s^R(\xi_s)]^{1/2} \xi_s$  or from  $\eta_s$  to  $m_s^R \eta_s$  in the usual energy variable<sup>37</sup>  $\eta_s$ , so that

$$\sigma_s^{\text{PWBAR}} = \sigma_s^{\text{PWA}} ([m_s^R(\xi_s)]^{1/2} \xi_s, \theta_s). \quad (7)$$

Although the weight functions  $W_s$  used in Eq. (5) were derived strictly in the slow collision limit ( $\xi_s \ll 1$ ), Eq. (7) still applies at higher velocities where the relativistic effect subsides. As shown in Figs. 1 and 2, our procedure yields cross sections that agree with the numerical calculations<sup>10-12, 25</sup> based on relativistic wave functions.

### III. POLARIZATION AND BINDING EFFECTS IN THE PERTURBED STATIONARY-STATE (PSS) THEORY

Atomic states are perturbed by the projectiles so as to influence the ionization cross section. In the adiabatic limit of very low velocities, the perturbed stationary states of the target electron become those of a diatomic molecule with a changing internuclear distance in the Born-Oppenheimer approximation. When  $Z_1 \ll Z_2$ , the impact parameters of importance for inner-shell ionization are so small that the electron states approach those of a united atom of atomic number  $Z_1 + Z_2$  which can then be treated simply in the plane-wave Born approximation. Such a treatment subsumes the binding effect and a relaxation of the inner-shell wave function. For  $K$  shells, this approach has been demonstrated to be useful as long as  $\xi_K < 0.25$ ,<sup>38</sup> subject to the restriction  $\omega_{2K} \ll E_1$  for the united atom  $Z_1 + Z_2$ .

Most low-velocity data are taken for  $K$  and  $L$  shells at larger  $\xi_s$  values, where the binding effect is the dominant consequence of PSS.<sup>1, 3</sup> At intermediate and high velocities, major contributions to the direct-ionization cross sections of an  $S$  shell come from distances larger than the shell radius. The particle, moving "outside" the  $S$  shell, perturbs this state which leads to the so called polarization effect.<sup>1, 14, 21, 39</sup> That is, at impact parameters larger than some value  $p_s$  comparable to  $a_{2s}$  the polarization effect results in *additive*  $Z_1^3$ -proportional terms which increase the cross sections. At impact parameters smaller than  $p_s$ , the binding effect yields, on the contrary, *subtractive*  $Z_1^3$ -proportional terms which decrease these cross sections.

The polarization effect was first invoked to explain stopping-power data.<sup>40</sup> The data show, relative to the  $Z_1^2$ -dependent Bethe theory,<sup>41</sup> an additional dependence on  $Z_1^3$ .<sup>42, 43</sup> Polarization terms of still higher order in  $Z_1$  are probably small.<sup>44</sup> The deviations from  $Z_1^2$  dependence signify that the first-Born approximation, on which Bethe's

derivation of stopping power is based, does not suffice. Inclusion of higher-order terms of the Born series leads to insurmountable difficulties unless advanced numerical procedures are used. Numerical coupled-state calculations have been performed heretofore only for the simplest projectile-target combinations, such as the proton-hydrogen system.<sup>45</sup> Other attempts to calculate inelastic collision cross sections have been made in the second-Born approximation<sup>46</sup> but have not led, as yet, to a methodological development for the calculation of inner-shell Coulomb ionization in the Born approximation higher than the first order ( $\propto Z_1^2$ ). Recently,  $K$ -shell vacancy production cross sections were calculated numerically with the first two terms in the Born series.<sup>47</sup> The results clearly corroborate the predictions of the theory<sup>14, 21</sup> which accounts for both the binding and polarization effects. Standard perturbation methods, although perhaps suitable for the calculation of polarization effects in elastic scattering, are inadequate when applied to inelastic collisions.<sup>48</sup> Eikonal approaches may account for the polarization effect when they are extended beyond the Glauber approximation,<sup>49</sup> but one is then faced with four-dimensional integrals, i.e., two more dimensions than needed in first-Born-approximation calculations.

We now proceed to develop a model approach to the polarization effect. Unperturbed atomic states are represented by isotropic harmonic oscillators in their ground state. The polarization of such oscillators by charged particles has been treated classically<sup>40</sup> and quantum mechanically<sup>50</sup> with identical results. Relativistic particles, not considered here, change these results only insignificantly.<sup>51</sup>

One calculates the energy transfer from a particle of charge  $Z_1$  and velocity  $v_1$ , at impact parameter  $p$  from the origin of an electron harmonic oscillator of frequency  $\omega$ . When integrated over the impact parameters larger than  $p_s$ , the mean energy transfer from such "distant collisions" including  $Z_1^3$ -proportional terms is<sup>40, 50</sup>

$$\Delta\omega(\omega) = \frac{4\pi Z_1^2}{v_1^2} \left( x_s K_0(x_s) K_1(x_s) + \frac{Z_1 \omega}{v_1^3} I(x_s) \right), \quad (8)$$

with  $x_s \equiv p_s \omega / v_1$ ,  $K_0$  and  $K_1$  being modified Bessel functions of the second kind. The  $Z_1^3$ -proportional first term of Eq. (8) results from the dipole component  $\propto R^{-2}$  of the particle-electron interaction,

$$-\frac{Z_1}{|\vec{R} - \vec{r}|} = -Z_1 \left[ \frac{1}{R} + \frac{\vec{R} \cdot \vec{r}}{R^3} + \frac{1}{2} \left( \frac{3(\vec{R} \cdot \vec{r})^2}{R^5} - \frac{r^3}{R^3} \right) + O\left(\frac{r^3}{R^4}\right) \right], \quad (9)$$

in the multiple expansion for  $R \gg r$ . The quadruple component  $\propto R^{-3}$  of the interaction polarizes the motion of the electron and results in the  $Z_1^3$ -proportional term in Eq. (8). The function  $I(x_s)$  is derived and displayed in Ref. 40 [cf. Eq. (10) and Figs. 1 and 2], and is used in considerations of  $Z_1^3$ -dependent stopping powers and ranges<sup>40,52</sup> as well as of  $Z_1^3$  effect for the energy loss of the ejected electrons.<sup>53</sup> An interpolation formula based on tables of  $I(x_s)$  accurate to within 1% is given by Eq. (27) of Ref. 14 for  $x_s \leq 3.1$ . To within 5%,  $I(x_s) = 2 \exp(-2x_s)/x_s^{1.6}$  for  $3 \leq x_s \leq 11$ .

"Close collisions," at  $p \leq p_s$ , may be regarded as binary encounters between the electrons and incident particles imparting momenta so large that the electrons behave as if they were free. Here, the contribution to the  $Z_1^3$  effect becomes negligible, because the Rutherford scattering is strictly proportional to  $Z_1^2$ .<sup>40</sup> The energy transfer in close collisions,  $(4\pi Z_1^2/v_1^2) \ln(p_s v_1^2/Z_1)$ , and in distant collisions,

$$\lim_{x_s \rightarrow 0} \frac{4\pi Z_1^2}{v_1^2} x_s K_0(x_s) K_1(x_s) = \frac{4\pi Z_1^2}{v_1^2} \ln \frac{1.123}{x_s},$$

add up to the classical formula of Bohr<sup>54</sup>

$$\Delta\omega^{\text{Bohr}}(\omega) = (4\pi Z_1^2/v_1^2) \ln(1.123 v_1^3/Z_1 \omega). \quad (10)$$

The connection to quantum mechanics was established by Bloch<sup>55</sup> with the result that

$$\Delta\omega^B(\omega) = (4\pi Z_1^2/v_1^2) \ln[2v_1^2 B(Z_1, v_1)/\omega], \quad (11)$$

where the function  $B(Z_1, v_1)$ , expressed in terms of the Euler  $\psi$  function

$$B(Z_1, v_1) \equiv \exp[\psi(1) - \text{Re} \psi(1 + i Z_1/v_1)], \quad (12)$$

takes the limiting forms

$$B(Z_1, v_1) = \begin{cases} \frac{1}{2}(1.123) v_1/Z_1 & \text{for } v_1 \ll Z_1, \\ 1 & \text{for } v_1 \gg Z_1, \end{cases} \quad (13)$$

independent of  $\omega$ . The limit  $v_1/Z_1 \gg 1$  of Eq. (11) is the quantum-mechanical Bethe formula.<sup>41</sup> When expanded in powers of  $Z_1/v_1$ , Eq. (12) contains only even powers of  $Z_1$ .

To make contact with atomic states, one invokes

$$\begin{aligned} g_K(\xi; c_K = 1.5) &= (1 + 9\xi + 31\xi^2 + 98\xi^3 + 12\xi^4 + 25\xi^5 + 4.2\xi^6 + 0.515\xi^7)/(1 + \xi)^9, \\ g_{L_1}(\xi; c_{L_1} = 1.5) &= (1 + 9\xi + 31\xi^2 + 49\xi^3 + 162\xi^4 + 63\xi^5 + 18\xi^6 + 1.97\xi^7)/(1 + \xi)^9, \\ g_{L_{2,3}}(\xi; c_{L_{2,3}} = 1.25) &= (1 + 10\xi + 45\xi^2 + 102\xi^3 + 331\xi^4 + 6.7\xi^5 + 58\xi^6 + 7.8\xi^7 + 0.888\xi^8)/(1 + \xi)^{10}. \end{aligned} \quad (19)$$

We join  $\epsilon_s^B(\xi_s, \theta_s; c_s)$  of Eq. (17) and  $\epsilon_s^P(\xi_s, \theta_s; c_s)$  of Eq. (16) into a PSS factor for  $\theta_s$ ,

$$\zeta_s(\xi_s, \theta_s; c_s) = 1 + (2Z_1/Z_{2s}\theta_s) \times [g_s(\xi_s; c_s) - h_s(\xi_s; c_s)]. \quad (20)$$

the fact that, for distant collisions, an atomic state can be described as an ensemble of harmonic oscillators.<sup>56</sup> Since the first-excited states of inner-shell electrons are close to the ionization edge, we set  $\omega = \omega_{2s}$ . We build the  $Z_1^3$ -proportional polarization of an atomic state into the theory by evaluating the mean energy transfer, Eq. (11), to a polarized state of frequency  $\epsilon_s \omega_{2s}$  so that

$$\Delta\omega^B(\epsilon_s \omega_{2s}) = \frac{4\pi Z_1^2}{v_1^2} \left[ \ln \frac{2v_1^2 B(Z_1, v_1)}{\omega_{2s}} + \frac{Z_1 \omega_{2s}}{v_1^3} I\left(\frac{p_s \omega_{2s}}{v_1}\right) \right]. \quad (14)$$

We define the polarization factor

$$\begin{aligned} \epsilon_s &= \exp\left[-\frac{Z_1 \omega_{2s}}{v_1^3} I\left(\frac{p_s \omega_{2s}}{v_1}\right)\right] \\ &= 1 - \frac{Z_1 \omega_{2s}}{v_1^3} I\left(\frac{p_s \omega_{2s}}{v_1}\right) + O(Z_1^2), \end{aligned} \quad (15)$$

which, to order  $(Z_1/v_1)^3$ , in our notation becomes

$$\epsilon_s^P(\xi_s, \theta_s; c_s) = 1 - (2Z_1/Z_{2s}\theta_s) h_s(\xi_s; c_s), \quad (16)$$

with

$$h_s(\xi_s; c_s) \equiv (2n_s/\theta_s \xi_s^3) I(c_s n_s/\xi_s),$$

where  $c_s \equiv p_s/a_{2s}$  is a cutoff constant of the order of unity.

The factor  $\epsilon_s^B$  accounts for the binding to the projectile when  $p < p_s$ , and can be written

$$\epsilon_s^B(\xi_s, \theta_s; c_s) = 1 + (2Z_1/Z_{2s}\theta_s) g_s(\xi_s; c_s), \quad (17)$$

where

$$g_s(\xi_s; c_s) \equiv \int_0^{c_s n_s/\xi_s} [\hat{\epsilon}_s(n_s \xi_s x) - 1] W_s(x) x dx, \quad (18)$$

with  $\hat{\epsilon}_s$  functions given by Eqs. (10) and (11) of Ref. 13.<sup>36</sup> We treat  $c_s$  as an adjustable parameter<sup>57</sup> and we find the best overall agreement with experiment by setting  $p_s = \langle r \rangle_s$ , where  $\langle r \rangle_s$  is the mean value of the radial distance in the  $S$  shell so that  $c_K = c_{L_1} = \frac{3}{2}$  and  $c_{L_2} = c_{L_3} = \frac{5}{4}$ . Suitable analytical approximations,<sup>58</sup> with errors less than 1%, are

In terms of  $\sigma_s^{\text{PWA}}$  of Eq. (1), the PSS cross section for direct ionization is given by

$$\sigma_s^{\text{PSS}} = \sigma_s^{\text{PWA}}(\xi_s/\xi_s, \xi_s \theta_s). \quad (21)$$

Similarly, we introduce  $\xi_s/\xi_s$  into Eq. (6) to

obtain the relativistic  $\xi_S$  correction appropriate for PSS, viz.,

$$\xi_S^R = [m_S^R(\xi_S/\zeta_S)]^{1/2} \xi_S. \quad (22)$$

Then, we get

$$\sigma_S^{\text{PSSR}} = \sigma_S^{\text{PWBA}}(\xi_S^R/\zeta_S, \xi_S \theta_S). \quad (23)$$

At large velocities,  $\xi_S \gg 1$ , one retrieves the PWBA for the unperturbed target atom.

#### IV. COULOMB-DEFLECTION EFFECT REVISITED

At low projectile velocities, the PWBA and the equivalent straight-line SCA can overestimate ionization cross sections by orders of magnitude because these descriptions neglect the influence of the internuclear repulsion. The repulsion slows down and deflects the projectile in the Coulomb field of the target nucleus. We refer to the consequences as the Coulomb-deflection effect, although it subsumes both the retardation and the deflection of the projectile in the field of the nucleus. Coulomb waves or Coulomb-deflected hyperbolic trajectories must be considered. Bang and Hansteen<sup>7</sup> treated the latter in the monopole-term approximation to the perturbing potential,

Eq. (9), and retained only the transitions to the  $l_f = 0$  final state of the electron in the continuum. The ratio of the differential ionization cross sections with respect to the final energy  $\mathcal{E}_f$  of the ejected electron calculated for the hyperbolic trajectory,  $(d\sigma_S/d\mathcal{E}_f)^{\text{hyp}}$ , and the straight-line trajectory,  $(d\sigma_S/d\mathcal{E}_f)^{\text{sl}}$ , determines the factor  $C \equiv (d\sigma_S/d\mathcal{E}_f)^{\text{hyp}}/(d\sigma_S/d\mathcal{E}_f)^{\text{sl}}$ . In the low-velocity limit,  $C$  was given as a complicated combination of modified Bessel functions of imaginary order and their derivatives.<sup>7</sup> Brandt *et al.*<sup>1-4, 13, 14, 21</sup> simplified this Coulomb-deflection factor to

$$C(x) = \exp(-\pi x), \quad (24)$$

where  $x \equiv \tau dq_{0S}$  is the product of the variable  $\tau \equiv 1 + \mathcal{E}_f/\omega_{2S}$ , the half-distance of closest approach in a head-on collision  $d \equiv Z_1 Z_2 / M v_1^2$ , with  $M^{-1} \equiv M_1^{-1} + M_2^{-1}$ , and  $q_{0S} \approx \omega_{2S}/v_1$ . The quantity  $dq_{0S}$ , which appears as  $\xi$  in studies of nuclear excitation,<sup>59</sup> is the ratio of the characteristic time in Coulomb scattering  $d/v_1$  to the electronic transition time  $1/\omega_{2S}$ , and so measures the adiabaticity of the collision.

The Coulomb-deflection factor has been evaluated numerically<sup>60-62</sup> and analytically.<sup>63</sup> Following Amundsen's approach,<sup>63</sup> we find (see Appendix A)

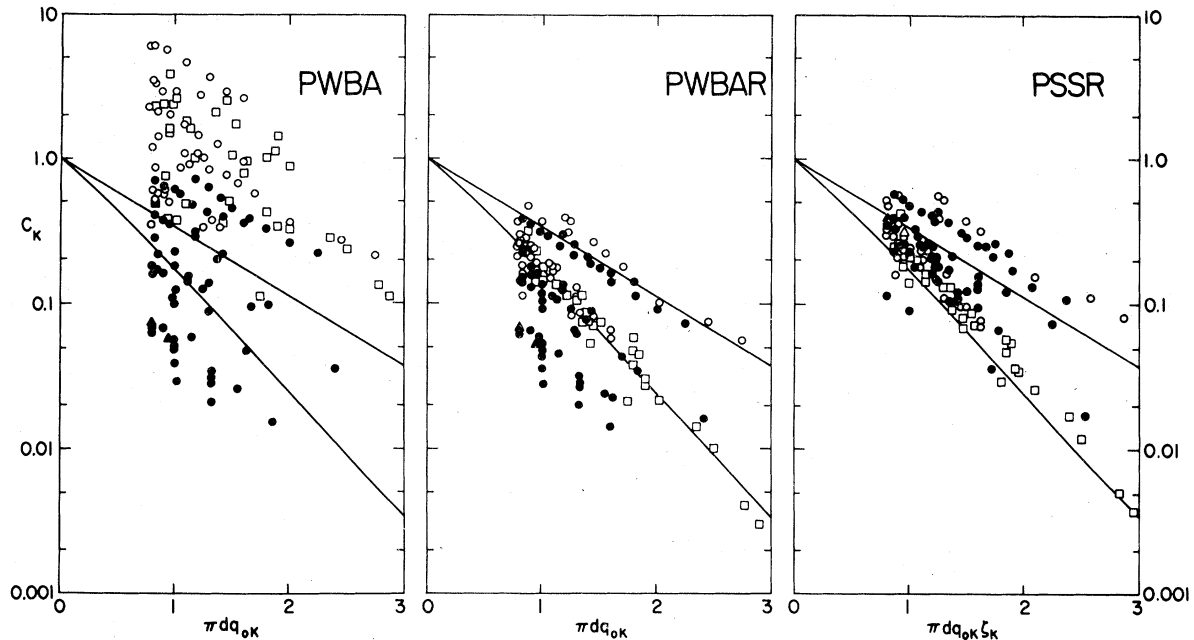


FIG. 3. Coulomb-deflection factor  $C_K$  for  $K$ -shell ionization, compared with  $\sigma_{KX}^{\text{EXPT}}/\sigma_{KX}^{\text{TH}}$ , i.e., the experimental x-ray production cross sections (Ref. 65) for protons (circles) and deuterons (triangles) are successively, from left to right, divided by the cross sections predicted in PWBA, PWBAR, and PSSR with the recent fluorescence yields (Ref. 70). Solid symbols are for  $Z_2 < 50$ , open symbols for  $Z_2 \geq 50$ . The curves for  $C_K$  are calculated with Eq. (24) (upper) and Eq. (25) (lower). As the theory improves, the locus of the data approaches the upper  $C_K$  curve, except for one set of measurements for protons (Ref. 68, open squares).

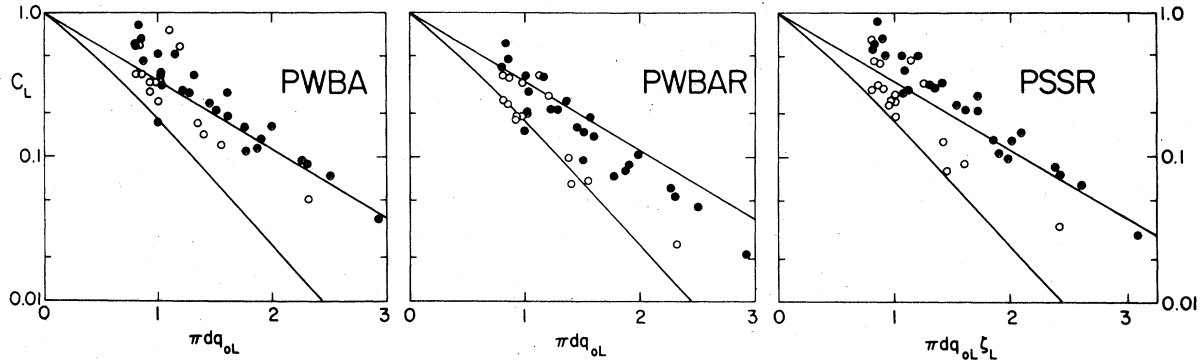


FIG. 4. Coulomb-deflection factor  $C_L$  for  $L$ -shell ionization compared with  $\sigma_{LX}^{\text{EXPT}}/\sigma_{LX}^{\text{TH}}$ , i.e., the experimental x-ray production cross sections (Ref. 66) for protons (circles) are successively, from left to right, divided by the cross sections predicted in PWBA, PWBAR, and PSSR with the recent fluorescence and Coster-Kronig yields (Ref. 70). Solid symbols are for  $Z_2 < 75$ , open symbols for  $Z_2 \geq 75$ . The abscissa values for the experimental points are mean values weighted according to the subshell cross sections. The curves for  $C_L$  are calculated with Eq. (24) (upper) and Eq. (25) (lower) for  $L_1$  subshell since  $L_2$  and  $L_3$  subshells do not contribute significantly at low velocities. As the theory improves, the locus of the data approaches the upper  $C_L$  curve.

$$C(x) = \exp(-\pi x) \left( x \frac{dK_{ix}(y)}{dy} \Big|_{y=x} \right)^2, \quad (25)$$

where  $K_{ix}(y)$  is the Bessel function of imaginary order. Equation (25) goes to Eq. (24) when  $x \ll 1$ . For  $x \sim 0.7$ , Eq. (25) agrees with the recent numerical calculations by Kocbach<sup>62</sup> and is smaller by a factor  $\sim 5$  than  $\exp(-\pi x)$ , Eq. (24), that was extracted and used by Brandt and his co-workers (see Fig. 11).

Before comparing  $C$  with experiment, one has to integrate over all values of  $\tau$ .<sup>2</sup> Since

$$\left( \frac{d\sigma}{d\mathcal{E}_f} \right)^{s1} \propto \left( \frac{1}{q_{oS}\tau} \right)^{10+2l_2} \quad (26)$$

in the slow-collision limit relevant for Coulomb deflection, the Coulomb-deflection factor for ionization of an S shell becomes

$$C_S(dq_{oS}) = \int_1^\infty \frac{C_\gamma(\tau dq_{oS}) d\tau}{\tau^{10+2l_2}}, \quad (27)$$

with  $l_2 = 0$  for  $S = K, L_1$  and  $l_2 = 1$  for  $S = L_2, L_3$ . Depending on  $C$ , Eq. (27) yields approximately

$$C_S(dq_{oS}) \simeq \frac{C_\gamma(dq_{oS})}{1 + \gamma \pi dq_{oS} / (9 + 2l_2)}, \quad (28)$$

where  $\gamma = 1$  if  $C_\gamma(dq_{oS})$  is given by Eq. (24) and  $\gamma = 2$  if given by Eq. (25) evaluated at  $\tau = 1$ .<sup>64</sup> In Figs. 3 and 4 we compare  $C_S$  with the ratio of experimental ionization cross sections<sup>65,66</sup> to theoretical predictions without the Coulomb-deflection effect. The ratios for  $K$ -shell ionization by protons and deuterons are based on the PWBA, Eq. (1), on the PWBAR, Eq. (7), and on the PSSR, Eq. (23). As one improves the theory through successive approximations, a locus of the data

marked as circles and triangles emerges that appears to follow the prediction of Eq. (27) with Eq. (24), i.e., that of Eq. (28) for  $\gamma = 1$ . A fit of some 3000 experimental  $K$ -shell ionization cross sections<sup>67</sup> to Eq. (28) implies  $\gamma = 1.17$ . By contrast, only the data (open squares) reported recently by Anholt<sup>68</sup> support Eq. (28) for  $\gamma = 2$  over the entire abscissa range. Inasmuch as Eq. (25) is accurate result of the monopole approximation in the expansion, Eq. (9), of the perturbing potential,<sup>69</sup> the experimental evidence suggests, on balance, that the dipole term and, perhaps, higher-order terms raise the Coulomb-deflection factor toward Eq. (24).

Figure 3 for  $K$  shells and Fig. 4 for  $L$  shells sum up the current status of experimental data. The serious dilemma they pose in deciding between theories of the Coulomb-deflection effect points to a crucial domain where new experiments are needed. For the present, we continue to employ Eq. (27), with Eq. (24) which is displayed as the upper curves in Figs. 3 and 4.

## V. COMPARISON WITH EXPERIMENT

In summary, we incorporate the Coulomb-deflection effect on the projectile ( $C$ ), the binding and polarization effects (PSS) and the relativistic effect ( $R$ ) on the target electron states into the theory for direct ionization of an S shell as

$$\sigma_S^{\text{PSSR}} = C_S(dq_{oS} \zeta_S) \sigma_S^{\text{PWBA}}(\xi_S^R / \zeta_S, \zeta_S \theta_S), \quad (29)$$

where  $C_S$  is given by Eq. (28) with  $\gamma = 1$ ,  $\xi_S^R$  by Eq. (22), and  $\zeta_S(\xi_S, \theta_S; c_S)$  by Eq. (20) setting  $c_S = 1.5$  and  $1.25$  for  $K, L_1$ , and for  $L_{2,3}$  shells, re-

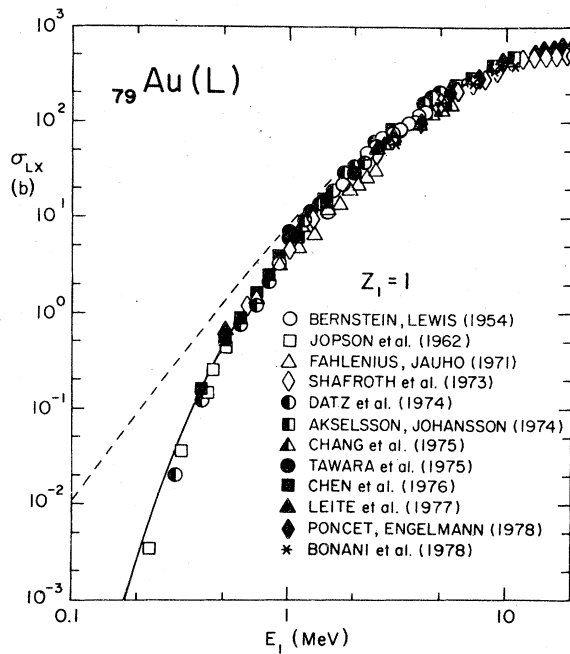


FIG. 5.  $L$ -shell x-ray production cross sections of  $^{79}\text{Au}$  for protons according to the PWBAR, Eq. (7) (dashed curve) and the CPSSR theory, Eq. (29) (solid curve). For comparison with experimental data (Ref. 71), the theoretical ionization cross sections were converted to x-ray production cross sections with the recent fluorescence and Coster-Kronig yields (Ref. 70).

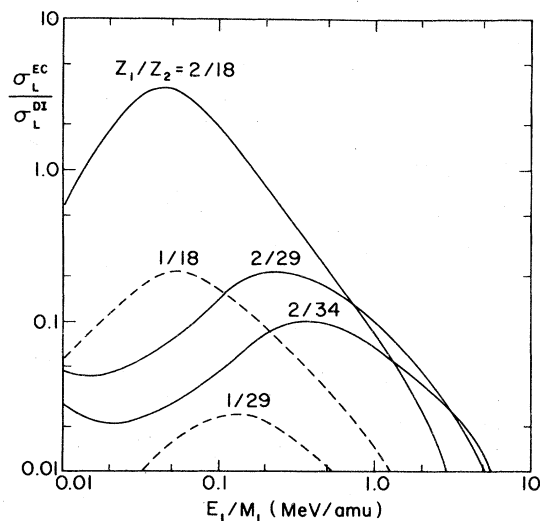


FIG. 6. Calculated ratios of cross sections for electron capture [ $\sigma_L^{\text{EC}}$  from Ref. 13] and direct ionization [ $\sigma_L^{\text{DI}}$  from Eq. (29)] for projectiles  $Z_1=1$  (dashed curves) and  $Z_1=2$  (solid curves) on the targets with the lowest atomic number  $Z_2$  for which  $L$ -shell ionization data are considered. Electron capture contributes significantly when  $Z_1/Z_2 > 0.1$ .

spectively. For comparisons with experimental x-ray and Auger-electron production cross sections, we convert the calculated ionization cross sections to the respective production cross sections with the aid of the fluorescence and Coster-Kronig yields that have recently been recommended by Krause.<sup>70</sup>

Figure 5 compares the predictions of PWBAR, according to Eq. (7) (dashed curve), and of CPSSR, according to Eq. (29) (solid curve), with  $L$ -shell x-ray production cross sections measured for protons on gold,<sup>71</sup> where  $Z_1/Z_2 = 0.013 \ll 1$ .

As  $Z_1/Z_2$  increases, electron capture into an unoccupied state of the projectile opens an additional channel for ionization. To account for this, we add to  $\sigma_S^{\text{PWBAR}}$  electron-capture (EC) cross sections that are based on Nikolaev's calculations<sup>72</sup> in the Oppenheimer-Brinkman-Kramers (OBK) approximation, which is a PWBA that neglects the internuclear interaction. And to  $\sigma_S^{\text{CPSSR}}$  we add the electron-capture cross sections according to Ref. 13.<sup>73</sup> The relativistic effect is included in these cross sections by analogy with the development given in Sec. II.<sup>74</sup>

For the  $Z_1=1$  and  $Z_1=2$  projectiles, the display in Fig. 6 illustrates that electron capture is not a significant process as long as  $Z_1/Z_2 < 0.1$ . This result pertains to all targets considered here, with the exception of  $^{18}\text{Ar}$  excited by  $^2\text{He}$  ions. As a converse example, we show in Fig. 7 a comparison for  $Z_1/Z_2 > 0.1$  between calculated  $L$ -x-ray production cross sections  $\sigma_{LX}^{\text{TH}}$  and experiments<sup>75-77</sup> for fully stripped  $^{19}\text{F}^{9+}$  ions  $\sigma_{LX}^{\text{EXPT}}$ .<sup>78</sup> The squares refer to the comparison with PWBAR, and the circles to the comparison with CPSSR. When electron capture is omitted (open symbols) the ratios  $\sigma_{LX}^{\text{TH}}/\sigma_{LX}^{\text{EXPT}}$  have a dependence on  $Z_1/Z_2$  and differ significantly from unity. When electron capture is included (closed symbols), the ratios become independent of  $Z_1/Z_2$  and, in the CPSSR approximation, are indeed equal to unity. As seen in Fig. 8, this approximation is also in satisfactory agreement with  $K$ -x-ray production data<sup>79</sup> for  $^{19}\text{F}$  ions moving in various solid targets at the same velocity with an equilibrated charge  $Z_1^* \approx 6.8$ .<sup>80</sup> Assuming that the projectile  $K$  shell is filled, electrons can be captured only in the essentially empty  $L$  shell and other higher shells. The electron capture cross sections are calculated accordingly. To distinguish them from cross sections for fully stripped ions (EC), they are labeled EC\*.

The number of  $L$ -shell x-ray production cross-section measurements with protons on gold has more than doubled since the publication of Fig. 1 in Ref. 4. As displayed in Fig. 5, they agree with the predictions of Eq. (29). To expand on the

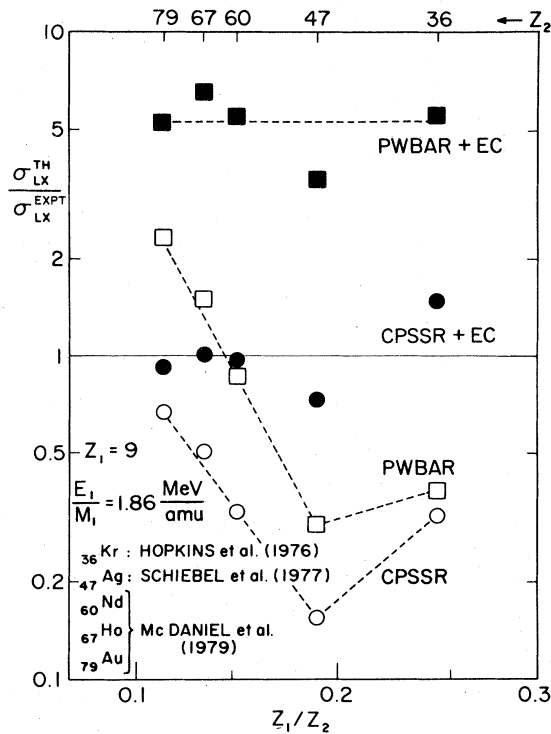


FIG. 7. Ratios of the theoretical and experimental cross sections for  $L$ -shell x-ray production by fully stripped  $^{13}\text{F}^{9+}$  ions of  $E_1 = 36$  MeV in  $^{36}\text{Kr}$  (Ref. 75), 35 MeV in  $^{47}\text{Ag}$  (Ref. 76), and 35.4 MeV in  $^{60}\text{Nd}$ ,  $^{67}\text{Ho}$ , and  $^{79}\text{Au}$  (Ref. 77) with fluorescence and Coster-Kronig yields according to Ref. 70. Squares: PWBAR; circles: CPSSR. Open symbols: direct ionization; closed symbols: electron capture added. Dashed lines are drawn to aid the eye. Within experimental uncertainties, closed circles (CPSSR + EC) follow the solid line marking the ideal ratio equal to one.

analysis for data obtained with protons ( $Z_1 = 1$ ) as shown in Fig. 4 of Ref. 4, we have compiled in a similar manner the data<sup>81</sup> for helium ions ( $Z_1 = 2$ ) on various elements in Fig. 9. Large discrepancies occur when these data are compared with  $\sigma_{LX}^{\text{PWBAR}}$  according to Eq. (7). The discrepancies are essentially accounted for by  $\sigma_{LX}^{\text{CPSSR}}$  according to Eq. (29).

The only remaining substantial disagreement between experiment and theory emerges for  $^{18}\text{Ar}$ . Multiple ionization in  $^{18}\text{Ar}$  by protons, and even more so by helium ions, increases the small x-ray fluorescence yield ( $\sim 2 \times 10^{-4}$ ) and thus raises the solid  $^{18}\text{Ar}$  curve toward the experimental data by perhaps as much as a factor of 5. The gap between the experiment and the theory, evaluated with the single- $L$ -hole fluorescence yields, can thus be understood as a measure of multiple vacancy formation in  $^2\text{He}-^{18}\text{Ar}$  collisions. But the

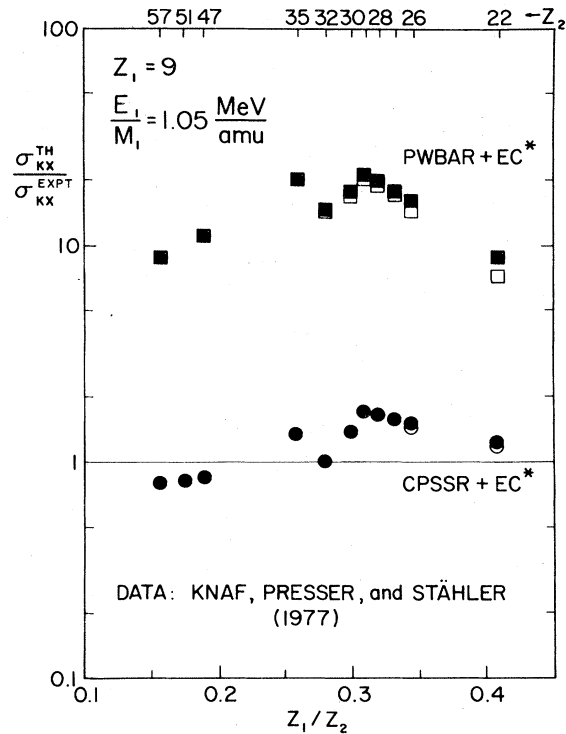


FIG. 8. Ratios of the theoretical and experimental cross sections for  $K$ -shell x-ray production by charge-equilibrated  $^{13}\text{F}$  ions of  $E_1 = 20$  MeV in  $^{22}\text{Ti}$ ,  $^{26}\text{Fe}$ ,  $^{27}\text{Co}$ ,  $^{28}\text{Ni}$ ,  $^{29}\text{Cu}$ ,  $^{30}\text{Zn}$ ,  $^{35}\text{Br}$ ,  $^{47}\text{Ag}$ ,  $^{51}\text{Sb}$ , and  $^{57}\text{La}$  (Ref. 79) with fluorescence yields according to Ref. 70. Symbols are as in Fig. 7, except that EC\* refers to electron capture by ions of effective charge (Ref. 80)  $Z_1^* = 0.76 \times 9$ .

fluorescence yields in heavier targets are insensitive to multiple ionization as discussed in Ref. 4. This observation, made earlier based on data with protons,<sup>4</sup> is supported here by the evidence obtained from  $^{29}\text{Cu}$  bombarded with helium ions.

Auger-electron production cross sections of  $^{18}\text{Ar}$   $L$  shells are not afflicted by these complications. Such data can be compared directly with the ionization theory [cf. Ref. 4, Eq. (27)] as is done in Fig. 10. The experimental cross sections<sup>82-85</sup> were measured with  $^1\text{H}$  and  $^4\text{He}$  ions as identified by closed and open symbols. In addition to the relativistic plane-wave Born approximation with electron capture (dashed curves: PWBAR + EC\*), the figure displays two sets of curves. One represents CPSSR calculated according to Eq. (29) (dashed-dot curves) and the other includes electron capture cross sections (solid curves). Electron capture is evaluated for the fraction of unoccupied states on the  $^1\text{H}$  and  $^4\text{He}$  projectiles as a function of velocity based on the charge states

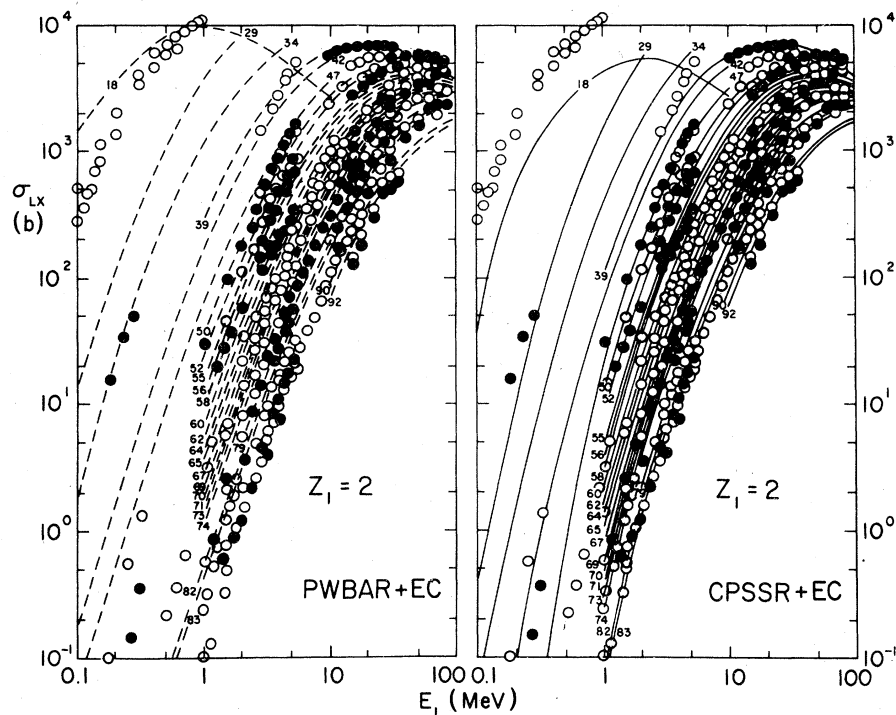


FIG. 9.  $L$ -shell x-ray production cross sections for 26 different targets for  ${}^4_2\text{He}$  ions. Dashed curves represent, Eq. (7); solid curves represent Eq. (29), both with appropriate electron-capture cross sections added. These ionization cross sections were converted to x-ray production cross sections using fluorescence and Coster-Kronig yields of Ref. 70. The curves are identified by the target atomic number  $Z_2$ . The experimental data (Ref. 81) are marked alternatively by open and closed circles for consecutive target elements, and can be recognized on the right-hand side.

in argon.<sup>86</sup> The data agree closely with the solid curves at the lowest energies and near the maxima, but otherwise fall below the curves by as much as a factor of 2. These deviations may be of systematic origin. They are relatively small when compared with data for protons on lighter gaseous targets, viz.,  ${}_{16}\text{S}$  and  ${}_{17}\text{Cl}$ .<sup>85,87</sup> The  ${}_{16}\text{S}$  cross sections<sup>87</sup> fall well below the predictions of the theory and nearly coincide with the  ${}_{18}\text{Ar}$  data, while, surprisingly, the  ${}_{17}\text{Cl}$  cross sections<sup>85</sup> are higher than the theoretical results. Proton<sup>88,89</sup> and helium data<sup>89</sup> for  ${}_{12}\text{Mg}$  and  ${}_{13}\text{Al}$  metals also are in disagreement with the theory. We may be on the trail of a new phenomenon here. It would, therefore, be desirable to extend the measurements of  $L$ -shell Auger-electron production cross sections to all elements in the third period over a wide energy range, to uncover systematic trends in this behavior.

This paper is the culmination of a program of study, set forth over a decade ago and developed systematically since.<sup>1-4,8,13,14,21</sup> The theory for the Coulomb excitation of inner shells has been formulated in a comprehensive manner to apply to all particle velocities. In the present paper, a procedure for including relativistic effects in the description of the target states is given and the effects of Coulomb repulsion between projectile and target nucleus are reassessed. The theory agrees in detail with the vast amount of data for  $Z_1/Z_2 \leq 0.3$ .

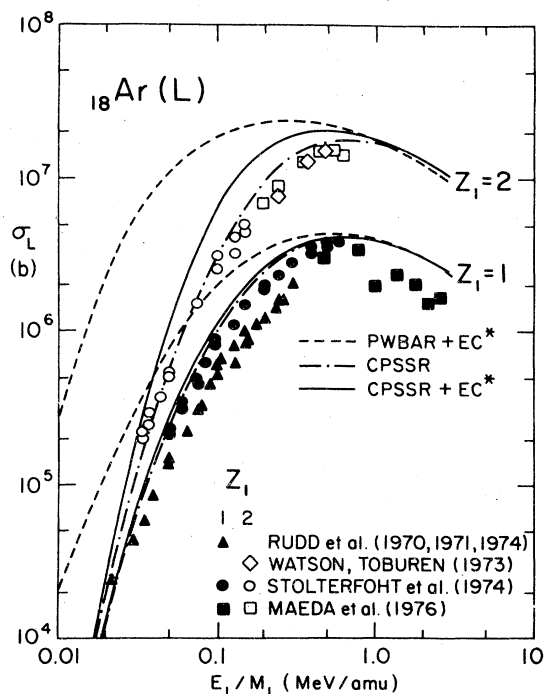


FIG. 10.  $L$ -shell ionization cross sections of  ${}_{18}\text{Ar}$  for  ${}^1_1\text{H}$  and  ${}^4_2\text{He}$  ions according to PWBAR, Eq. (7), with electron capture (EC\*) by the ion in the velocity-dependent charge state added (dashed curves); according to CPSSR, Eq. (29) (dash-dotted curves), and EC\* added (solid curves). They are compared with experimental Auger-electron production cross sections (Refs. 82-85); closed symbols:  ${}^1_1\text{H}$  ions, open symbols:  ${}^4_2\text{He}$  ions.

The discussion emphasizes three areas in need of new investigations. The empirical Coulomb-deflection factors scatter widely and may even bifurcate so as to follow distinct predictions that can differ by as much as an order of magnitude. Systematic measurements in the difficult range of very low particle velocities should resolve such inconsistencies in the present data, while the theoretical attack on this problem ought to continue. Furthermore, large discrepancies appear in the  $L$ - $x$ -ray production cross sections when  $Z_1/Z_2$  exceeds  $\sim 0.3$ . These discrepancies are important because they may be invoked to determine the increase in the fluorescence yields due to multiple ionizations. Such yields can be calculated and be tested independently, provided that Auger data become available to establish the range of applicability for the Coulomb-ionization theory when  $Z_1/Z_2 \geq 0.3$ . Finally, the elements in the third period of the Periodic Table pose new challenges: the as yet sparse Auger data show bizarre trends when gauged by the  $Z_2$  dependence of the theory. The  $L$  shell in this group of elements is the outermost closed shell of the ion cores, and the gaps between inner-shell ionization theory and Auger

data may signify new chemical and morphological effects which warrant exploration.

*Note added in proof.* Since this paper went to press, new  $L$ -shell data have been published<sup>90</sup> which can be compared with the theory.

#### ACKNOWLEDGMENT

This work was supported by the U. S. Department of Energy.

#### APPENDIX A: COULOMB DEFLECTION IN THE MONOPOLE APPROXIMATION

In considering ionization from the  $1s$  ground state to the  $s$  wave in the continuum, Amundsen<sup>63</sup> concluded that the atomic form factor can be factored out from the Bang-Hansteen matrix element, and thus does not affect the Coulomb deflection factor

$$C(x) \equiv \frac{(d\sigma_s/d\mathcal{E}_f)^{\text{hvp}}}{(d\sigma_s/d\mathcal{E}_f)^{\text{st}}} \approx e^{-\pi x} \int_0^\infty p dp K_{ix}^2(\epsilon x) / \int_0^\infty p dp K_0^2\left(\frac{px}{d}\right), \quad (\text{A1})$$

where  $\epsilon \equiv [1 + (p/d)^2]^{1/2}$ ;  $x$  is defined in connection with Eq. (24). One has<sup>91</sup>

$$2 \int_1^\infty d\epsilon \in K_{ix}(\epsilon x) K_{ix}(\epsilon x) = 2 \int_1^\infty d\epsilon \in K_{ix}(\epsilon x) K_{-ix}(\epsilon x) = \epsilon x^2 [K_{ix}(\epsilon x) K_{-ix}(\epsilon x) - K_{1+ix}(\epsilon x) K_{1-ix}(\epsilon x)] \Big|_{\epsilon=1}^{\epsilon=\infty} = x^2 [K_{1+ix}(x) K_{1-ix}(x) - K_{ix}^2(x)] = \left( x \frac{d}{dy} K_{ix}(y) \Big|_{y=x} \right)^2, \quad (\text{A2})$$

so that

$$C(x) = \exp(-\pi x) \left( x \frac{d}{dy} K_{ix}(y) \Big|_{y=x} \right)^2. \quad (\text{A3})$$

Although a tabulation of  $K_{ix}(x)$  exists for  $0.2 \leq x \leq 50$ ,<sup>92</sup> we could not find tables of  $(d/dy)K_{ix}(y)$  that would be needed for the evaluation of Eq. (A3). In the  $x \rightarrow 0$  limit,  $K_{ix}(y)|_{y=x} = -\ln x$ , and one retrieves

$$C(x) = \exp(-\pi x), \quad x \ll 1. \quad (\text{A4})$$

This is the factor, Eq. (24), used by Brandt *et al.*<sup>1-4, 13, 14, 21</sup> As shown in Fig. 11, it agrees with the numerical calculations of Kocbach<sup>61</sup> for  $x < 0.2$ . In the  $x \rightarrow \infty$  limit, one can evaluate the integral representation

$$K_{ix}(y) = \frac{1}{2 \cosh(\frac{1}{2}\pi x)} \int_{-\infty}^{\infty} e^{iys \sinh t} \cos xt \, dt \quad (\text{A5})$$

by the method of steepest descent with  $\sinh t \approx t + t^3/3! + \dots$ . The leading term becomes

$$K_{ix}(y) = \frac{\pi}{2 \cosh(\frac{1}{2}\pi x)} \left( \frac{2}{y} \right)^{1/3} \text{Ai}(z), \quad y \gg 1, \quad (\text{A6})$$

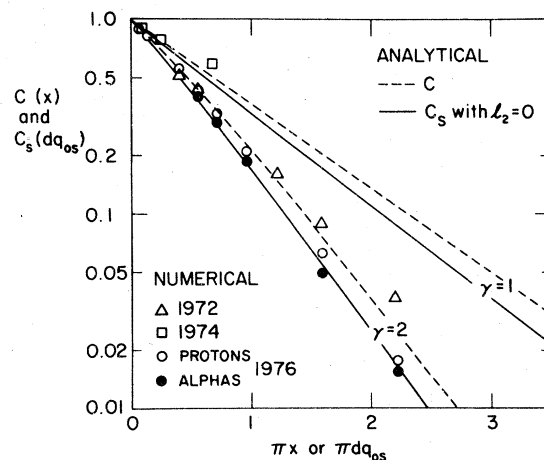


FIG. 11. Theoretical Coulomb-deflection factors in the monopole approximation before integration,  $C(x)$  (dashed curves), and after integration  $C_s(dq_{0s})$  (solid curves), over final electron energies. The upper two curves represent Eqs. (24) and (28) for  $\gamma=1$ ,  $l_2=0$ ; the lower two curves represent Eqs. (25) and (28) for  $\gamma=2$  and  $l_2=0$ . Numerical results are from Ref. 60 ( $\Delta$  1972), Ref. 61 ( $\square$  1974), and Ref. 62 ( $\circ$  protons and  $\bullet$   $\alpha$  particles 1976).

where  $z \equiv 2^{1/3}(y^{2/3} - x/y^{1/3})$  and Ai is the Airy function.<sup>93</sup> Since  $dz/dy|_{y=x} = (2/x)^{1/3}$  and  $\text{Ai}(z) \simeq [3^{2/3}\Gamma(\frac{2}{3})]^{-1} - z[3^{1/3}\Gamma(\frac{1}{3})]^{-1}$  when  $z \ll 1$ , we obtain  $C(x)$  to the leading term as

$$C(x) \simeq \frac{5}{3} x^{2/3} \exp(-2\pi x), \quad x \gg 1. \quad (\text{A7})$$

Guided by this asymptotic form, we find that

$$C(x) = (1 - \frac{1}{3}x^{1/3} + \frac{5}{3}x^{2/3}) \exp(-2\pi x) \quad (\text{A8})$$

approximates the results of our numerical integration of Eq. (A1) to within 3%. Kocbach's numerical results for  $C$  are slightly higher for protons than for  $\alpha$  particles.<sup>62</sup> To the extent that this additional projectile dependence varies with  $Z_1/M_1$ , and all projectiles fall into the range  $\frac{1}{2} \leq Z_1/M_1 \leq 1$ , we estimate that such an extra dependence would change Eq. (A3) by at most  $\sim 10\%$ .

#### APPENDIX B: SAMPLE CALCULATION OF L-SHELL X-RAY PRODUCTION CROSS SECTIONS

Detailed quantitative assessments of theories relative to experiment require that measured cross sections are reported in tabular form. We illustrate the scheme of cross-section calculations for  $\alpha$  particles ( $Z_1=2, M_1=4 \text{ amu} = 4 \times 1836 m$ ) impinging with  $E_1=1 \text{ MeV}$  and  $E_1=80 \text{ MeV}$  on gold ( $Z_2=79, M_2=197 \text{ amu}$ ) with the observed binding energies<sup>22</sup> 14.35, 13.73, and 11.92 keV for the  $L_1, L_2$ , and  $L_3$  subshells, respectively. The corresponding values of  $\theta_{L_i}$  are 0.735, 0.721, and 0.625. With  $n_2=2$  and the screened nuclear charge  $Z_{2L} = 79 - 4.15 = 74.85$ , one has  $a_{2L} = 4/74.85 = 0.05344$ ,  $v_{2L} = 74.85/2 = 37.425$ . Since  $8\pi a_0^2 = 7.04 \times 10^8 b$ , Eq. (1) reads

$$\sigma_{L_i}^{\text{PWBA}} = (2)1435b \times F_{L_i}(\xi_{L_i}, \theta_{L_i})/\theta_{L_i}, \quad (\text{B1})$$

where the factor (2) applies only for the  $L_3$  sub-

TABLE I.  $L$ -shell ionization cross sections (in barns) and quantities required for their evaluation. The numerical values pertain to the sample calculation delineated in Appendix B for 1- and 80-MeV  $\alpha$  particles on gold.

$E_1$ $v_1/v_{2L}$ Quantity	${}^4_2\text{He}^{2+} \rightarrow {}^{197}_{79}\text{Au}(L)$			$Z_{2L} = 74.85$ $a_{2L} = 0.5344 \text{ a.u.}$ $v_{2L} = 37.425 \text{ a.u.}$			$\theta_{L_1} = 0.753$ $\theta_{L_2} = 0.721$ $\theta_{L_3} = 0.625$
	$L_1$	1 MeV 0.0847 $L_2$	$L_3$	80 MeV 0.759 $L_1$	$L_2$	$L_3$	Eq. or Ref.
$\xi_{L_i}$	0.225	0.235	0.271	2.02	2.11	2.43	Eq. (2)
$m_{L_i}^R(\xi_{L_i})$	1.303	1.210	1.180	1.030	1.021	1.019	Eq. (6)
$(m_{L_i}^R)^{1/2} \xi_{L_i} \equiv X$	0.257	0.259	0.294	2.05	2.13	2.45	Eq. (7)
$F_{L_i}(X, \theta_{L_i})$	$4.33 \times 10^{-4}$	$9.46 \times 10^{-5}$	$2.55 \times 10^{-4}$	0.840	0.799	0.906	Refs. 4 and 21
$\sigma_{L_i}^{\text{PWBA}}[b]$	0.825	0.188	1.171	$1.60 \times 10^3$	$1.59 \times 10^3$	$4.16 \times 10^3$	Eqs. (7) and (B1)
$g_{L_i}$	0.903	0.991	0.987	0.328	0.177	0.137	Eq. (19)
$h_{L_i}$	0	0	0	0.037	0.088	0.110	Eq. (16)
$g_{L_i} - h_{L_i}$	0.903	0.991	0.987	0.291	0.089	0.027	
$\zeta_{L_i}$	1.063	1.073	1.084	1.021	1.007	1.002	Eq. (20)
$\xi_{L_i}/\zeta_{L_i}$	0.211	0.219	0.250	1.98	2.10	2.43	
$m_{L_i}^R(\xi_{L_i}/\zeta_{L_i})$	1.326	1.227	1.197	1.031	1.022	1.019	Eq. (6)
$\xi_{L_i}^R/\zeta_{L_i}$	0.243	0.243	0.274	2.01	2.12	2.45	
$\zeta_{L_i} \theta_{L_i}$	0.801	0.774	0.678	0.769	0.726	0.626	
$F_{L_i}(\xi_{L_i}^R/\zeta_{L_i}, \zeta_{L_i} \theta_{L_i})$	$3.20 \times 10^{-4}$	$5.74 \times 10^{-5}$	$1.47 \times 10^{-4}$	0.831	0.794	0.906	Refs. 4 and 21
$\sigma_{L_i}^{\text{PSSR}}[b]$	0.573	0.106	0.622	$1.55 \times 10^3$	$1.57 \times 10^3$	$4.15 \times 10^3$	Eqs. (23) and (B1)
$\pi dq_{0L_i} \xi_{L_i}$	1.22	1.18	1.03	0.002	0.002	0.001	Eq. (B2)
$C_{L_i}$	0.260	0.278	0.326	0.998	0.998	0.999	Eq. (28) with $\gamma=1$
$\sigma_{L_i}^{\text{CPSSR}}[b]$	0.149	0.029	0.203	$1.55 \times 10^3$	$1.57 \times 10^3$	$4.15 \times 10^3$	Eq. (29)

shell. With  $M^{-1} \equiv M_1^{-1} + M_2^{-1} = 0.000139$ , the argument of the Coulomb-deflection factor,  $\pi dq_{oL_i} \xi_{Li}$  of Eq. (29), is

$$3.14 \times \frac{Z_1 Z_2}{M v_1^2} \times \frac{\frac{1}{8} Z_{2L}^2 \theta_{Li} \xi_{Li}}{v_1} = \frac{48.3 \theta_{Li} \xi_{Li}}{v_1^3}. \quad (\text{B2})$$

Here  $v_1 = 3.17$  and  $28.4$  for the 1- and 80-MeV  $\alpha$  particles. These values are chosen to demonstrate the importance of the relativistic, binding, and Coulomb-deflection effects in slow collisions ( $v_1/v_{2L} = 0.0847$ ) on the one hand, and, on the other, the significance of the polarization effect when the projectile velocity becomes comparable to  $v_{2L}$  ( $v_1/v_{2L} = 0.759$ ).

We calculate  $\sigma_{Li}^{\text{PWBAR}}$  and  $\sigma_{Li}^{\text{CPSSR}}$  as displayed in Table I. These direct-ionization cross sections can be compared at once with the x-ray production data since the electron capture contributes less than 1% of ionization for  $Z_1/Z_2 = 0.025 \ll 1$ . We employ recently recommended x-ray emission probabilities<sup>70</sup> 0.330, 0.373, and 0.320 for the L subshells of gold. The L-shell x-ray production

cross sections are

$$\begin{aligned} \sigma_{LX}^{\text{PWBAR}} &= (0.330 \times 0.825 + 0.373 \times 0.188 \\ &\quad + 0.320 \times 1.171)b = 0.726b, \quad (\text{B3}) \\ \sigma_{LX}^{\text{CPSSR}} &= (0.330 \times 0.149 + 0.373 \times 0.029 \\ &\quad + 0.320 \times 0.203)b = 0.125b \end{aligned}$$

for 1-MeV  $\alpha$  particles, and

$$\begin{aligned} \sigma_{LX}^{\text{PWBAR}} &= (0.330 \times 1600 + 0.373 \times 1590 \\ &\quad + 0.320 \times 4160)b = 2450b, \\ \sigma_{LX}^{\text{CPSSR}} &= (0.330 \times 1550 + 0.373 \times 1570 \\ &\quad + 0.320 \times 4150)b = 2430b \end{aligned} \quad (\text{B4})$$

for 80-MeV  $\alpha$  particles. Corresponding experimental values are  $(0.10 \pm 0.02)b$  (Ref. 94) and  $(0.16 \pm 0.04)b$  (Ref. 95) for 1 MeV, and  $(2810 \pm 140)b$  (Ref. 96) and  $(2710 \pm 250)b$  (Ref. 97) for 80-MeV  $\alpha$  particles.

<sup>1</sup>(a) W. Brandt, in *Proceedings of the International Conference on Inner Shell Ionization Phenomena and Future Applications, Atlanta, Georgia, 1972*, edited by R. W. Fink, S. T. Manson, M. Palms, and P. V. Rao (U.S. AEC, Oak Ridge, Tenn., 1973), p. 948; (b) in *Atoms 3, Proceedings of the Third International Conference on Atomic Physics, Boulder, Colorado, 1972*, edited by S. T. Smith, C. K. Walters, and L. H. Volsky (Plenum, New York, 1973), p. 155.

<sup>2</sup>W. Brandt, R. Laubert, and I. Sellin, *Phys. Lett.* **21**, 518 (1966); *Phys. Rev.* **151**, 56 (1966).

<sup>3</sup>G. Basbas, W. Brandt, and R. Laubert, *Phys. Rev. A* **7**, 983 (1973).

<sup>4</sup>W. Brandt and G. Lapicki, *Phys. Rev. A* **10**, 474 (1974).

<sup>5</sup>H. A. Bethe, in *Handbuch der Physik*, edited by A. Smekal (Springer, Berlin, 1933), Vol. 24/1, p. 273.

<sup>6</sup>G. S. Khandelwal, B.-H. Choi, and E. Merzbacher, *At. Data* **1**, 103 (1969); the L-shell tables were superseded by B.-H. Choi, E. Merzbacher, and G. S. Khandelwal, *ibid.* **5**, 291 (1973); the K-shell tables were extended by R. Rice, G. Basbas, and F. D. McDaniel, *At. Nucl. Data* **20**, 503 (1977).

<sup>7</sup>J. Bang and J. M. Hansteen, *K. Dan. Vidensk. Selsk. Mat. Fys. Medd.* **31**, No. 13 (1959); J. M. Hansteen and O. P. Mosebekk, *Z. Phys.* **234**, 281 (1970); J. M. Hansteen, *Adv. At. Mol. Phys.* **11**, 299 (1975).

<sup>8</sup>G. Basbas, W. Brandt, and R. H. Ritchie, *Phys. Rev. A* **7**, 1971 (1973).

<sup>9</sup>This implies that the relativistic correction to the kinetic projectile energy is less than 2%. For relativistic projectiles see D. M. Davidović, B. L. Moiseiwitsch, and P. H. Norrington, *J. Phys. B* **11**, 847 (1978); R. Anholt, *Phys. Rev. A* **19**, 1004 (1979); B. L. Moiseiwitsch and P. H. Norrington, *J. Phys. B* **12**, L283 (1979).

<sup>10</sup>D. Jamnik and Č. Zupančič, *K. Dan. Vidensk. Selsk. Mat. Fys. Medd.* **31**, No. 2 (1957); T. Mukoyama and L. Sarkadi, *Bull. Inst. Chem. Res., Kyoto Univ.* **57**, 33 (1979).

<sup>11</sup>B.-H. Choi, *Phys. Rev. A* **4**, 1002 (1971); and in Ref. 1(a), p. 1093.

<sup>12</sup>P. A. Amundsen, *J. Phys. B* **9**, 971 (1976); **9**, 2163(E) (1976); **10**, 1097 (1977). Inner-shell ionization cross sections were calculated by Amundsen in the straight-line semiclassical approximation which is equivalent to the PWBA.

<sup>13</sup>G. Lapicki and W. Losonsky, *Phys. Rev. A* **15**, 896 (1977); F. D. McDaniel, J. L. Duggan, G. Basbas, P. D. Miller, and G. Lapicki, *ibid.* **16**, 1375 (1977).

<sup>14</sup>G. Basbas, W. Brandt, and R. Laubert, *Phys. Rev. A* **17**, 1655 (1978).

<sup>15</sup>When the single-electron approximation is made, calculations of inner-shell ionization cross sections include the possibility of a simultaneous ionization of other shells [J. F. Reading, *Phys. Rev. A* **8**, 3262 (1973); J. H. McGuire and J. R. Macdonald, *ibid.* **11**, 146 (1975); and G. Basbas, *Bull. Am. Phys. Soc.* **20**, 675 (1975)].

<sup>16</sup>G. Basbas and G. S. Khandelwal, *Bull. Am. Phys. Soc.* **11**, 307 (1966); G. Basbas, Ph.D. thesis (North Carolina University, Chapel Hill, 1968) (unpublished); M. Pauli, F. Rösler, and D. Trautmann, *Phys. Lett.* **67A**, 28 (1978).

<sup>17</sup>G. Basbas, *Bull. Am. Phys. Soc.* **14**, 631 (1969); **16**, 564 (1971).

<sup>18</sup>S. T. Manson, *Phys. Rev. A* **6**, 1013 (1972).

<sup>19</sup>K. G. Baur, Q. Fazly, H. Mommsen, P. Schürkes, and M. Pauli, *Phys. Lett.* **68A**, 223 (1978).

<sup>20</sup>B.-H. Choi, *Phys. Rev. A* **11**, 2004 (1975); F. F. Komarov and A. P. Novikov, *Zh. Tekh. Fiz.* **48**, 1449 (1978) [*Sov. Phys. Tech. Phys.* **23**, 819 (1978)].

- <sup>21</sup>G. Lapicki, Ph.D. thesis (New York University, New York, 1975) (unpublished).
- <sup>22</sup>J. A. Bearden and A. Burr, *Rev. Mod. Phys.* **39**, 125 (1967).
- <sup>23</sup>H. W. Lewis, B. E. Simmons, and E. Merzbacher, *Phys. Rev.* **91**, 943 (1953); Č. Zupančič and T. Huus, *ibid.* **94**, 205 (1954).
- <sup>24</sup>P. D. Miller, Masters thesis (Rice University, Houston, 1956); G. Basbas, *Bull. Am. Phys. Soc.* **13**, 80 (1968); C. B. O. Mohr, *Adv. At. Mol. Phys.* **4**, 221 (1968).
- <sup>25</sup>M. Pauli, F. Rösler, and D. Trautmann, *J. Phys. B* **11**, 2511 (1978).
- <sup>26</sup>E. Merzbacher and H. W. Lewis, in Ref. 5, edited by S. Flügge, 1958, Vol. 34, p. 166.
- <sup>27</sup>T. L. Hardt and R. L. Watson, *Phys. Rev. A* **7**, 1917 (1973).
- <sup>28</sup>J. S. Hansen, *Phys. Rev. A* **8**, 822 (1973); Addendum (1973, unpublished).
- <sup>29</sup>P. A. Amundsen, L. Kocbach, and J. M. Hansteen, *J. Phys. B* **9**, L203 (1976); **9**, 2755(E) (1976).
- <sup>30</sup>E. Caruso and A. Cesati, *Phys. Rev. A* **15**, 432 (1977).
- <sup>31</sup>H. Hönl, *Z. Phys.* **84**, 1 (1933).
- <sup>32</sup>A. Berinde, C. Deberth, I. Neamu, C. Protop, N. Scintei, V. Zoran, M. Dost, and S. Röhl, *J. Phys. B* **11**, 2875 (1978).
- <sup>33</sup>R. Anholt, *Phys. Rev. A* **17**, 976 (1978).
- <sup>34</sup>T. Huus, J. H. Bjerregaard, and B. Elbek, *K. Dan. Vidensk. Selsk. Mat. Fys. Medd.* **30**, No. 17 (1956).
- <sup>35</sup>M. E. Rose and T. A. Welton, *Phys. Rev.* **86**, 432 (1952).
- <sup>36</sup>See Eq. (16) of Ref. 4. The function  $W_{L_2, L_3}$  is in error in this reference and should be replaced by Eq. (A10), Ref. 13, viz.,  $W_{L_2, 3}(x) = \frac{1}{192} x^6 [K_2^2(x) + K_3^2(x)]$ . A different form of this function was obtained by R. P. Singhal and V. Singh [*Physica (Utr.)* **83C**, 200 (1976)] because they included  $l_f=0$  and 1 for final angular momentum states of the ejected electron; however, only the  $l_f=0$  state contributes in the low-velocity limit. Also,  $\hat{\epsilon}_{L_i}$  for  $L_{2,3}$  given by Eq. (14) in Ref. 4 contains an error. The correct value of  $c_{L_2, 3}$  appearing in this equation is 3 [see Eq. (11) of Ref. 13].
- <sup>37</sup>See Eq. (3.13) of Ref. 26; in our notation,  $\eta_S = (\theta_S \xi_S / 2n_S)^2$ .
- <sup>38</sup>J. U. Andersen, E. Laegsgaard, M. Lund, and C. D. Moak, *Nucl. Instrum. Methods* **132**, 507 (1976); and E. Laegsgaard, J. U. Andersen, and M. Lund, in *Invited Talks, Tenth International Conference on Physics of Electronic and Atomic Collisions, Paris, 1977*, edited by G. Watel (North-Holland, Amsterdam, 1978), p. 353.
- <sup>39</sup>G. Basbas, W. Brandt, and R. Laubert, *Phys. Lett.* **34A**, 277 (1971); G. Basbas, W. Brandt, R. Laubert, A. Ratkowski, and A. Schwarzschild, *Phys. Rev. Lett.* **27**, 171 (1971).
- <sup>40</sup>J. C. Ashley, R. H. Ritchie, and W. Brandt, *Phys. Rev. B* **5**, 2392 (1972).
- <sup>41</sup>H. A. Bethe, *Ann. Phys. (Leipz.)* **5**, 325 (1930).
- <sup>42</sup>W. H. Barkas, W. Birnbaum, and F. M. Smith, *Phys. Rev.* **101**, 778 (1956); W. H. Barkas, J. N. Dyer, and H. H. Heckman, *Phys. Rev. Lett.* **11**, 26 (1963); **11**, 138(E) (1963); H. H. Heckman and P. J. Lindstrom, *ibid.* **22**, 871 (1969), and references cited therein.
- <sup>43</sup>H. H. Andersen, H. Simonsen, and H. Sørensen, *Nucl. Phys. A* **125**, 171 (1969); L. E. Porter and C. L. Shepard, *Nucl. Instrum. Methods* **117**, 1 (1974); R. Ishiwari, N. Shiomi, and S. Shiari, *Phys. Lett. A* **51**, 53 (1975); S. Datz, J. Gomez del Campo, P. F. Dittner, P. D. Miller, and J. A. Biggerstaff, *Phys. Rev. Lett.* **38**, 1145 (1977); H. H. Andersen, J. F. Bak, H. Knudsen, and B. R. Nielsen, *Phys. Rev. A* **16**, 1929 (1977); L. E. Porter, *Nucl. Instrum. Methods* **148**, 119 (1978); **157**, 333 (1978).
- <sup>44</sup>G. Basbas, W. Brandt, and R. H. Ritchie, *Bull. Am. Phys. Soc.* **22**, 487 (1977); R. H. Ritchie and G. Basbas, *ibid.* **22**, 609 (1977); R. H. Ritchie and W. Brandt, *Phys. Rev. A* **17**, 2102 (1978).
- <sup>45</sup>See, for example, R. Shakeshaft, *Phys. Rev. A* **14**, 1626 (1976); **18**, 1930 (1978).
- <sup>46</sup>W. Rothenstein, *Proc. Phys. Soc. (London)* **67**, 673 (1954); A. E. Kingston, B. L. Moiseiwitsch, and B. G. Skinner, *Proc. R. Soc. A* **258**, 237 (1960); **258**, 245 (1960); B. L. Moiseiwitsch and P. Perrin, *Proc. Phys. Soc. (London)* **85**, 51 (1965); A. R. Holt and B. L. Moiseiwitsch, *J. Phys. B* **2**, 36 (1968); and *Adv. At. Mol. Phys.* **4**, 143 (1968); A. R. Holt, *J. Phys. B* **2**, 1202 (1969); M. J. Woolings and M. R. C. McDowell, *ibid.* **5**, 1220 (1972); **6**, 450 (1973); D. Baye and P.-H. Heenen, *ibid.* **6**, 105 (1973); H. R. J. Walters, *Comm. At. Mol. Phys.* **5**, 173 (1976); A. C. Yates, *Phys. Rev. A* **19**, 1550 (1979).
- <sup>47</sup>J. F. Reading, A. L. Ford, and E. Fitchard, *Phys. Rev. Lett.* **36**, 573 (1976); and *Phys. Rev. A* **16**, 133 (1977).
- <sup>48</sup>C. B. O. Mohr, *J. Phys. B* **8**, 388 (1975).
- <sup>49</sup>R. J. Glauber, in *Lectures in Theoretical Physics*, edited by W. E. Brittin *et al.* (Interscience, New York, 1959); E. Gerjuoy and B. K. Thomas, *Rep. Prog. Phys.* **37**, 1345 (1974); J. Bienstock and J. F. Reading, *Phys. Rev. A* **11**, 1205 (1975); J. E. Golden and J. H. McGuire, *ibid.* **12**, 80 (1975).
- <sup>50</sup>K. W. Hill and E. Merzbacher, *Phys. Rev. A* **9**, 156 (1974).
- <sup>51</sup>J. D. Jackson and R. L. McCarthy, *Phys. Rev. B* **6**, 4131 (1972). Note, however, that this change may become significant when  $Z_1 \geq 20$  [P. B. Eby and S. H. Morgan, Jr., *Phys. Rev. A* **5**, 2536 (1972); S. Ahlen, *ibid.* **17**, 1236 (1978)].
- <sup>52</sup>J. C. Ashley, R. H. Ritchie, and W. Brandt, *Phys. Rev. A* **8**, 2408 (1973); and **10**, 737 (1974); W. Brandt and R. H. Ritchie, *Nucl. Instrum. Methods* **172**, 41 (1976).
- <sup>53</sup>J. H. Miller, *Phys. Rev. A* **16**, 2478 (1977).
- <sup>54</sup>N. Bohr, *Philos. Mag.* **25**, 10 (1913).
- <sup>55</sup>F. Bloch, *Ann. Phys. (Leipz.)* **16**, 285 (1933).
- <sup>56</sup>E. J. Williams, *Proc. R. Soc. A* **139**, 163 (1933).
- <sup>57</sup>We recall that Bloch (Ref. 55) chose  $\langle r \rangle$  in the Thomas-Fermi atom as the dividing impact parameter between close and distant collisions in stopping powers. In the correspondence limit, the wave functions of the hydrogenic atom go over into harmonic-oscillator wave functions which peak near the radius  $(n_2/\omega_2 S)^{1/2} = \sqrt{2} a_{2S}/(n_2 \theta_S)^{1/2}$  [cf. R. Rockmore, *Am. J. Phys.* **43**, 29 (1975)]. Since  $(n_2 \theta_S)^{1/2}$  is close to one, it follows that the appropriate value for  $p_S$  is  $\sim \sqrt{2} a_{2S}$ . The discussions in Refs. 40, 44, and 50 in fact advocate such a choice for  $p_S$ .

- <sup>58</sup>The coefficients 9 and 10 preceding  $\xi$  in Eq. (19) were chosen to ensure that  $1 - g_S(\xi_S; c_S) \propto \xi_S^2$  for small  $\xi_S$ . The coefficient preceding the highest power of  $\xi_S$  was determined by analytical integration of Eq. (18) with the exact forms for  $W_S$ ; the remaining coefficients were obtained by least-squares fits to the results of numerical integration for  $g_S(\xi_S; c_S)$ .
- <sup>59</sup>See, for example, K. Alder and A. Winther, *Electromagnetic Excitation Theory of Coulomb Excitation with Heavy Ions* (North-Holland, Amsterdam, 1975).
- <sup>60</sup>K. Brunner, Ph.D. thesis (Würzburg University, Würzburg, 1972) (unpublished); K. Brunner and W. Hink, *Z. Phys.* **262**, 181 (1973).
- <sup>61</sup>L. Kocbach, *Phys. Fenn.* **9**, Suppl. S1. **46** (1974).
- <sup>62</sup>L. Kocbach, *Phys. Norvegica* **8**, 187 (1976).
- <sup>63</sup>P. A. Amundsen, *J. Phys. B* **10**, 2177 (1977).
- <sup>64</sup>This equation approximates the results of the numerical integration for  $\gamma=2$  to within a few percent, just as  $\exp(-\pi\xi)/(1 + \frac{1}{9}\pi\xi)$  approximates  $C_K(\xi) = 9E_{10}(\pi\xi)$  for  $\gamma=1$ .
- <sup>65</sup>Following are the references to the K-shell x-ray production cross sections by protons and deuterons ( $Z_1=1$ ) that are included in Fig. 3; the data that are not shown and referenced are those for which the argument  $dq_{oK}$  of  $C_K$  is less than 0.25. The numbers in the square brackets after each reference are the atomic numbers  $Z_2$  of the target atoms: P. R. Bevington and E. M. Bernstein, *Bull. Am. Phys. Soc.* **1**, 198 (1956) [92]; J. M. Hansteen and S. Messelt, *Nucl. Phys.* **2**, 526 (1957) [29, 42]; E. Merzbacher and W. Lewis in *Ref. 26* [82]; S. Messelt, *Nucl. Phys.* **5**, 435 (1958) [26, 29, 42, 47, 50, 73]; R. C. Jopson, H. Mark, and C. D. Swift, *Phys. Rev.* **127**, 1612 (1962) [22, 40]; J. M. Khan and D. L. Potter, *ibid.* **133**, A890 (1964) [29]; J. M. Khan, D. L. Potter, and R. D. Worley, *ibid.* **139**, A1735 (1965) [12, 13]; W. Brandt, R. Laubert, and I. A. Sellin, in *Ref. 2* [13]; W. Brandt and R. Laubert, *Phys. Rev.* **178**, 225 (1969) [13]; K. G. Harrison, H. Tawara, and F. J. DeHeer, *Physica (Utr.)* **66**, 16 (1973) [18]; G. Basbas, W. Brandt, and R. Laubert, in *Ref. 3* [13]; K. Brunner and W. Hink, *Z. Phys.* **262**, 181 (1973) [13]; T. L. Criswell and T. J. Gray, *Phys. Rev. A* **10**, 1145 (1974) [42]; N. A. Khelil and T. J. Gray, *ibid.* **11**, 893 (1975) [50, 51, 52, 57]; V. S. Nikolaev, V. P. Petukhov, E. A. Romanovsky, V. A. Sergeev, I. M. Kruglova, and V. V. Beloshitsky, in *Physics of Electronic and Atomic Collisions: Invited Lectures, Review Papers, and Progress Reports of the IX International Conference on the Physics of Electronic and Atomic Collisions, Seattle, July 1975*, edited by J. S. Risle and R. Gaballe (University of Washington, Seattle, 1976), p. 419 [30]; S. R. Wilson, F. D. McDaniel, J. R. Rowe, and J. L. Duggan, *Phys. Rev. A* **16**, 903 (1977) [47, 53, 58, 59, 60, 63, 64]; M. Kamiya, K. Ishii, K. Sera, S. Morita, and H. Tawara, *ibid.* **16**, 2295 (1977) [67, 79, 92]; O. Benka and M. Geretschlager, *Z. Phys. A* **284**, 29 (1978) [29, 47]; C. Bauer, R. Mann, and W. Rudolph, *ibid.* **287**, 27 (1978) [47].
- <sup>66</sup>Following are the references to the L-shell x-ray production cross sections by protons ( $Z_1=1$ ) that are included in Fig. 4; the data that are not shown and referenced are those for which the argument  $dq_{oL}$  of  $C_L$  is less than 0.25. The numbers in the square brackets after each reference are the atomic numbers  $Z_2$  of the target atoms: R. C. Jopson, H. Mark, and C. D. Swift, *Phys. Rev.* **127**, 1612 (1962) [73, 78, 79, 80, 82, 83, 92]; K. Shima, I. Makino, and M. Sakisaka, *J. Phys. Soc. Jpn.* **30**, 611 (1971) [42, 47]; C. E. Busch, A. B. Baskin, P. H. Nettles, S. M. Shafroth, and A. W. Waltner, *Phys. Rev. A* **7**, 1601 (1973) [82]; S. Datz, J. L. Duggan, L. C. Feldman, E. Laegsgaard, and J. U. Andersen, *ibid.* **9**, 192 (1974) [79]; F. Abrath and T. J. Gray, *ibid.* **10**, 1157 (1974) [66]; C. N. Chang, J. F. Morgan, and S. L. Blatt, *ibid.* **11**, 607 (1975) [73, 79, 83]; J. R. Chen, J. D. Reber, D. J. Ellis, and T. E. Miller, *ibid.* **13**, 941 (1976) [79]; C. V. B. Leite, N. V. DeCastro Faria, and A. G. DePinho, *ibid.* **15**, 943 (1977) [81, 82, 83, 90, 92]; R. M. Wheeler, R. P. Chaturvedi, and S. Amey, *Bull. Am. Phys. Soc.* **23**, 1060 (1978) [59, 62, 65, 70].
- <sup>67</sup>A. Langenberg and J. van Eck, *J. Phys. B* **10**, L419 (1977); and A. Langenberg (private communication, 1977).
- <sup>68</sup>R. Anholt, *Phys. Rev. A* **17**, 983 (1978).
- <sup>69</sup>P. A. Amundsen, *J. Phys. B* **11**, 3197 (1978); O. Aashamar, P. A. Amundsen, and L. Kocbach, *Phys. Lett.* **67A**, 349 (1978).
- <sup>70</sup>M. O. Krause, *J. Phys. Chem. Ref. Data* **8**, 307 (1979).
- <sup>71</sup>E. M. Bernstein and H. W. Lewis, *Phys. Rev.* **95**, 83 (1954); R. C. Jopson, H. Mark, and C. D. Swift, *ibid.* **127**, 1612 (1962); A. Fahlenius and P. Jauho, *Ann. Acad. Sci. Fenn.* **A6**, No. 367, 3 (1971); S. M. Shafroth, G. A. Bissinger, and A. W. Waltner, *Phys. Rev. A* **7**, 566 (1973); S. Datz, J. L. Duggan, L. C. Feldman, E. Laegsgaard, and J. U. Andersen, *ibid.* **9**, 192 (1974); R. Akselsson and T. B. Johansson, *Z. Phys.* **266**, 245 (1974); C. N. Chang, J. F. Morgan, and S. L. Blatt, *Phys. Rev. A* **11**, 607 (1975); H. Tawara, K. Ishii, S. Morita, H. Kaji, and T. Shiokawa, *ibid.* **11**, 1560 (1975); J. R. Chen, J. D. Reber, D. J. Ellis, and T. E. Miller, *ibid.* **13**, 941 (1976); J. R. Chen, *Nucl. Instrum. Methods* **142**, 9 (1977); C. V. Leite, N. V. deCastro Faria, and A. G. de Pinho, *Phys. Rev. A* **15**, 943 (1977); M. Poncet and C. Engelmann, *Nucl. Instrum. Methods* **149**, 461 (1978); G. Bonani, C. Stoller, M. Stöckli, M. Suter, and W. Wöflfi, *Helv. Phys. Acta* **51**, 272 (1978).
- <sup>72</sup>V. S. Nikolaev, *Zh. Eksp. Teor. Fiz.* **51**, 1263 (1966) [*Sov. Phys. JETP* **24**, 847 (1967)].
- <sup>73</sup>Equation (20) of Ref. 13 is approximated by Eq. (50) of Ref. 14 to within 30% for the collision systems considered in Ref. 14. This approximation may lead to errors when applied to other systems. For them, Eq. (20) of Ref. 13 should be consulted.
- <sup>74</sup>In the electron-capture cross sections Refs. 13 and 72, one replaces  $v_1^2$  with  $m_S^R(\xi_{SS})v_1^2$ , where  $m_S^R$ , Eq. (6), is evaluated at  $\xi_{SS}(\epsilon_S^R\theta_S) \equiv v_{2S}/[v_{1S}^2 + q_{2S}^2(\epsilon_S^R\theta_S)^2]^{1/2}$  with  $\epsilon_S^R$  of Eq. (17) or  $\epsilon_S^R=1$  in Nikolaev's calculations. Here,  $q_{SS}(\theta_S) \equiv \frac{1}{2}[v_1 + (v_{2S}^2\theta_S - v_{1S}^2)/v_1]$  is the minimum momentum transfer to an  $S'$  shell on the projectile where the captured electron has the orbital velocity  $v_{1S'} \equiv Z_1/n_1$ .
- <sup>75</sup>F. Hopkins, R. Brem, A. R. Whitemore, N. Cue, V. Dutkiewicz, and R. P. Chaturvedi, *Phys. Rev. A* **13**, 74 (1976).
- <sup>76</sup>U. Schiebel, T. J. Gray, R. K. Gardner, and P. Richard, *J. Phys. B* **10**, 2189 (1977).

- <sup>77</sup>F. D. McDaniel, A. Toten, R. S. Peterson, J. L. Duggan, S. R. Wilson, J. D. Gresset, P. D. Miller, and G. Lapicki, *Phys. Rev. A* **19**, 1517 (1979).
- <sup>78</sup>The  $^{13}\text{Ar}$  data ( $Z_1/Z_2=0.5$ ) of Ref. 75 are not shown in Fig. 7 because the fluorescence yield ( $2 \times 10^{-4}$ ) can change by as much as two orders of magnitude.
- <sup>79</sup>B. Knaf, G. Presser, and J. Stähler, *Jahresbericht 1977, Dynamitron-Tandem-Laboratorium Bochum-Dortmund-Münster*, edited by E. Kuhlmann and G. Presser (Bochum, West Germany, 1977) (unpublished), p. 45; *Z. Phys. A* **289**, 131 (1979).
- <sup>80</sup>W. Brandt, in *Atomic Collisions in Solids*, edited by S. Datz, B. R. Appleton, and C. D. Moak (Plenum, New York, 1975), Vol. 1, p. 261; B. S. Yarlagadda, J. E. Robinson, and W. Brandt, *Phys. Rev. B* **17**, 3475 (1978).
- <sup>81</sup>Following are the references to the  $L$ -shell x-ray production cross sections by helium ions ( $Z_1=2$ ) that are included in Fig. 9. The numbers in the square brackets after each reference are the atomic numbers  $Z_2$  of the target atoms: B. Singh, *Phys. Rev.* **108**, 1449 (1957) [47]; P. Komarek, *Acta. Phys. Austriaca* **27**, 369 (1968) [34, 42, 47, 50, 58, 62, 74, 79, 82, 83]; R. L. Watson, C. W. Lewis, and J. B. Natowitz, *Nucl. Phys. A* **154**, 561 (1970) [50, 69, 73, 79]; F. W. Saris, *Physica (Utr.)* **52**, 290 (1971) [18]; K. Shima, I. Makino, and M. Sakisaka, *J. Phys. Soc. Jpn.* **31**, 971 (1971) [29, 42, 47]; R. McKnight, S. T. Thornton, and R. C. Ritter, in Ref. 1a, p. 1439 [62, 73]; K.-H. Schartner, H. Schafer, and P. Hippler, *J. Phys. B* **7**, L111 (1974) [18]; N. Stolterfoht and D. Schneider (private communication, 1974) [18]; S. T. Thornton, R. H. McKnight, and R. R. Karlowicz, *Phys. Rev. A* **10**, 219 (1974) [47, 50, 65, 79, 83]; R. G. Flocchini, Ph. D. thesis (University of California at Davis, 1974) (unpublished), [55, 56, 58, 64, 69, 71, 82, 90, 92]; F. Folkmann, J. Borggreen, and A. Kjeldgaard, *Nucl. Instrum. Methods* **119**, 117 (1974) [60, 69, 82]; C. N. Chang, J. F. Morgan, and S. L. Blatt, *Phys. Rev. A* **11**, 607 (1975) [73, 79, 83]; T. Gray, G. M. Light, R. K. Gardner, and F. D. McDaniel, *ibid.* **12**, 2393 (1975) [70, 82]; T. L. Hardt and R. L. Watson, *ibid.* **14**, 137 (1976) [50, 52, 58, 69, 79, 82]; P. Baeri, S. V. Campisano, G. Immé, E. Rimini, and G. Della Mea, *Nucl. Instrum. Methods* **149**, 435 (1978) [52, 82]; M. Poncet and C. Engelmann, *ibid.* **149**, 461 (1978) [39, 50, 55, 58, 62, 67, 74, 79].
- <sup>82</sup>D. J. Volz and M. E. Rudd, *Phys. Rev. A* **2**, 1395 (1970); J. B. Crooks and M. E. Rudd, *ibid.* **3**, 1628 (1971); M. E. Rudd, *ibid.* **10**, 518 (1974).
- <sup>83</sup>R. L. Watson and L. H. Toburen, *Phys. Rev. A* **7**, 1853 (1973).
- <sup>84</sup>N. Stolterfoht, D. Schneider, and P. Ziem, *Phys. Rev. A* **10**, 81 (1974); N. Stolterfoht (private communication, 1974).
- <sup>85</sup>N. Maeda, N. Kobayashi, H. Hori, and M. Sakisaka, *J. Phys. Soc. Jpn.* **40**, 1430 (1976).
- <sup>86</sup>S. K. Allison, *Rev. Mod. Phys.* **30**, 1137 (1958); L. I. Pivovarov, V. M. Tubaev, and M. T. Novikov, *Zh. Eksp. Teor. Fiz.* **41**, 26 (1961) [*Sov. Phys. JETP* **14**, 20 (1962)].
- <sup>87</sup>L. H. Toburen, W. E. Wilson, and L. E. Porter, *J. Chem. Phys.* **67**, 4212 (1977).
- <sup>88</sup>C. J. Powell, R. J. Stein, P. B. Needham, Jr., and T. J. Driscoll, *Phys. Rev. B* **16**, 1370 (1977).
- <sup>89</sup>C. Benazeth, N. Benazeth, and L. Viel, *Surf. Sci.* **65**, 165 (1977); C. Benazeth, Ph.D. thesis (Université Paul Sabatier, Toulouse, 1977) (unpublished).
- <sup>90</sup>M. R. Khan, A. G. Hopkins, and D. Crumpton, *Z. Phys. A* **288**, 133 (1978); S. Hagmann, P. Armbruster, G. Kraft, P. H. Mokler, and H.-J. Stein, *ibid.* **288**, 353 (1978); K. G. Bauer, Q. Fazly, H. Mommsen, and P. Schürkes, *J. Phys. B* **11**, 4227 (1978); H. Kojima, N. Kobayashi, N. Maeda, and M. Sakisaka, *J. Phys. Soc. Jpn.* **46**, 198 (1979); M. Poncet and C. Engelmann, *Nucl. Instrum. Methods* **159**, 455 (1979).
- <sup>91</sup>Amundsen's formula  $C(x) = \pi x e^{-\pi x} / \sinh(\pi x)$  is the result of a mistaken integration from  $\epsilon=0$  (instead of  $\epsilon=1$ ) to  $\epsilon=\infty$  in Eq. (3.7) of Ref. 63.
- <sup>92</sup>S.-K. Luke and S. Wiessman, "Bessel functions of imaginary order and imaginary argument," University of Maryland, 1964. (Defense Documentation Center for Scientific and Technical Information, Cameron Station, Alexandria, Virginia) (unpublished).
- <sup>93</sup>*Handbook of Mathematical Functions*, edited by M. Abramowitz and I. A. Stegun (Dover, New York, 1965), p. 446.
- <sup>94</sup>S. T. Thornton, R. H. McKnight, and R. R. Karlowicz, *Phys. Rev. A* **10**, 219 (1974).
- <sup>95</sup>C. N. Chang, J. F. Morgan, and S. L. Blatt, *Phys. Rev. A* **11**, 607 (1975).
- <sup>96</sup>R. L. Watson, C. W. Lewis, and J. B. Natowitz, *Nucl. Phys. A* **154**, 561 (1970).
- <sup>97</sup>T. L. Hardt and R. L. Watson, *Phys. Rev. A* **14**, 137 (1976).